

1

2 Prof. Jim Freer

3 Editor

4 Hydrology and Earth System Sciences

5

May 18th, 2015

6 Dear Prof. Freer,

7

8 We would like to acknowledge the revision of our work entitled “**Propagation of hydro-**
9 **meteorological uncertainty in a model cascade framework to inundation prediction**”. Again, we
10 thank you for your constructive comments.

11 We have digested the concerns from the reviewer and added some new information to clarify these
12 points. We believe that this new version of our manuscript is indeed better and thank the reviewers and
13 yourself for your effort and time in this revision. In the following lines we explain how (i.e. by writing
14 our reply in red) and where (i.e. by giving line numbers) the raised points have been addressed in the
15 revised manuscript. We hope that this new version proves to be worth for publication in HESS.

16

17 Best wishes,

18

19

20 Dr. Adrián Pedrozo-Acuña on behalf of all authors

21

22

1 **Editor Decision: Publish subject to minor revisions (Editor review)**

2 Comments to the Author: The paper is now getting close to be acceptable for publication. However the
3 2nd reviewer has identified some omissions and also some inconsistencies which need to be addressed
4 before this happens. These should not add too much to the paper length but the justification for
5 differences in model skill has to be scientifically justified and the overall aims of the uncertainty
6 cascade and what it does and doesn't do. So if the authors can address these points, respond and
7 complete the modifications necessary we should be able to move to publication, best wishes, Jim

8

9 Reviewer 3: Propagation of hydro-meteorological uncertainty in a model cascade framework to
10 inundation prediction – REVIEW

11 This paper considers the propagation of uncertainty through a cascading model system, linking a
12 Numerical Weather Prediction model with hydrological and 2D hydrodynamic models. The paper is
13 well written and the topic will be of interest to a wide ranging audience, although I am not entirely
14 sure what specifically this work contributes to scientific progress. **This should be more clearly**
15 **specified by the authors.**

16 **R: In order to provide a clearer specification of the contribution of our work, we have modified the**
17 **abstract and conclusions to highlight its overall purpose.**

18 **In the abstract, we have acknowledged this fact in the following manner, at Page 1 in particular adding**
19 **the sentences shown here in bold:**

20 “This investigation aims to study the propagation of meteorological uncertainty within a cascade
21 modelling approach to flood prediction. The methodology was comprised of a Numerical Weather
22 Prediction Model (NWP), a distributed rainfall-runoff model and a 2D hydrodynamic model. **The**
23 **quantification of uncertainty was carried out in a hindcast scenario, removing non-behavioural**
24 **ensemble members at each stage, based on the fit with observed data.** The selected extreme event
25 corresponds to a flood that took place in the Southeast of Mexico during November 2009, for which
26 field data (e.g. rain gauges; discharge) and satellite imagery were available. Uncertainty in the
27 meteorological model was estimated by means of a multi-physics ensemble technique, which
28 considers variations in the specific setup options to determine a given precipitation. Precipitation fields
29 from the meteorological model were employed as input in a distributed hydrological model, and
30 resulting flood hydrographs were used as forcing conditions in the 2D hydrodynamic model. **This**
31 **enabled the assessment of uncertainty and its propagation, from a modelled rainfall event to a**
32 **predicted flooded area and depth.** Moreover, the evolution of skill within the model cascade shows
33 a complex aggregation of errors between models, suggesting that in valley-filling events hydro-
34 meteorological uncertainty has a larger effect on inundation depths than that observed in estimated
35 flood inundation extents.”

36

37 In this resubmission, the paper has been substantially improved and the authors have addressed many
38 of the previous reviewers’ comments adequately, although I do have some questions:

39

1 The research aims to quantify uncertainty in a hindcast scenario, removing non-behavioural ensemble
2 members at each stage based on the fit with observed data. In the first instance (NWP predictions), a
3 Nash Sutcliffe (NS) value of >0.3 is accepted as behavioural, while the hydrographs were rejected if
4 the score fell below 0.6. How were these limits defined? Justification should be given, particularly as
5 the choices that are made will have a significant influence on the perceived uncertainty in the model
6 chain.

7 **R:** We thank the reviewer for this comment. It should be noted that the change in the spatial scale from
8 the meteorological model to the distributed hydrological model, involves some sort of downscaling
9 issue. Transferring information from a large scale (atmospheric domain) to a smaller scale
10 (catchment), involves downscaling and in this sense, we modified the model performance criteria for
11 the hydrologic model to consider only the members with $NSC > 0.6$. The more relaxed criteria used at
12 the NWP stage is thought in order to incorporate predictions with a wide range of skill, from which the
13 error may be propagated to both the hydrologic and hydrodynamic scale of the model chain.

14 The uncertainty in the hydrological model parameters are defined by calibrating the model to a series
15 of past events. Some more information would be useful. For instance, what rainfall input was used
16 during this calibration?

17 **R:** The utilised rainfall input corresponds to that recorded for those events at the same 4 weather
18 stations that are within the river catchment, which location is shown in the top panel of Figure 1. This
19 has been acknowledged in Page 11 Line 30 to Page 12 Line 2.

20 Also, what was the advantage in defining 6 sets of parameter values from various events rather than
21 simply using the 2009 event and accepting any parameter sets that provided hydrographs that lay
22 within the specified threshold? This is particularly relevant as some of the calibrated NS scores were
23 very poor (e.g. 0.155), while also the 2009 event was significantly larger than any of the others.

24 **R:** In the hydrological model, the definition of six sets of plausible parameters from past flood events
25 (Table 3) is thought to reduce the dimensionality of the parameter calibration problem (see Gupta et
26 al., 2009). This procedure was preferred over a GLUE analysis, as the investigation was aimed to the
27 understanding of the propagation of uncertainty along the model chain. In other words, to evaluate
28 how an error originated in the meteorological model propagates to the definition of an inundated area
29 and depth. Although simplistic, it is important to report on how an error originated in the first model
30 of the chain is propagated to a result of interest to decision-makers (flood map).

31 On the other hand, it is reflected that the use of six sets of parameters from past flood events enable a
32 multi-response validation, which in due course allow the assessment of the overall modelling
33 performance. Additionally, it should be borne in mind that there are too many sources of uncertainty in
34 the modelling process within a cascade of models that cannot easily be disaggregated. Thus, it is
35 necessary to make assumptions about how to represent uncertainty, and there are sufficient degrees of
36 freedom in doing so, such that different methods based on different types of assumptions (including
37 purely qualitative evaluations) cannot easily be accepted or rejected.

38

39 There is no representation of uncertainty in the hydrodynamic model. This feels like a fairly major
40 omission given the attempt to establish a framework for quantifying uncertainty in extreme events.
41 There are many sources of uncertainty in hydrodynamic models, and I feel the exclusion of all of them

1 needs some further justification. Alternatively, could sensible parameter ranges be estimated using a
2 Monte Carlo approach, rejecting parameter ranges based on NS scores as done for the other model
3 components?

4 **R:** As the reviewer points out, there are many sources of uncertainty that arise in producing fluvial
5 flood risk maps. Some of these have to do with the natural variability in the occurrence of floods;
6 others have more to do with the limited knowledge available about the nature of flood runoff and flood
7 wave propagation including the geometry and infrastructure of flood plains.

8 Indeed, several investigations confirm that there is significant uncertainty associated with flood extent
9 predictions using hydraulic models (e.g. Aronica et al., 1998, 2002; Bates et al. 2004; Pappenberger et
10 al., 2005, 2006, 2007; Romanowicz and Beven, 2003). These uncertainties may be ascribed to
11 differences in spatio-temporal resolutions used in the numerical model, or the hydraulic roughness that
12 is determined for the river and flood plain; and little guidance exists on the magnitude of such effects.
13 This opens the door to complex questions of scaling and dimensionality. However, in our study, a
14 more detailed consideration of the different sources of uncertainty in the hydraulic model was not
15 pursued, this is due to the fact that the numerical setup of the hydraulic model is built following
16 published guidelines for an accurate representation of our problem (see Asselman et al. 2008).

17 For instance, high quality topographic and bathymetric data were employed (LiDAR derived DEM
18 and field survey) for the construction of the numerical representation of both, the river and the
19 floodplain. It is reflected that this enables us to build the discussion on how an uncertainty generated at
20 the meteorological stage of the model chain propagates and influences a resulting flooded area and
21 depth.

22 This justification has been included in the manuscript at Page 15 Line 1 – Line 10.

23 Complementary references that have been included:

24 Aronica, G, Hankin, B.G., Beven, K.J., 1998, Uncertainty and equifinality in calibrating distributed
25 roughness coefficients in a flood propagation model with limited data, *Advances in Water Resources*,
26 22(4), 349-365

27 Aronica, G., Bates, P.D. and Horritt, M.S., 2002. Assessing the uncertainty in distributed model
28 predictions using observed binary pattern information within GLUE. *Hydrological Processes*, 16,
29 2001- 2016.

30 Asselman, N., Bates P., Woodhead S., Fewtrell T., Soares-Frazão S., Zech Y., Velickovic M., de Wit
31 A., ter Maat J., Verhoeven G., Lhomme J. 2008. Flood Inundation Modelling – Model Choice and
32 Proper Application, Report T08-09-03, FLOODsite Project.

33 Bates, P. D., Horritt, M. S., Aronica, G. and Beven, K J, 2004, Bayesian updating of flood inundation
34 likelihoods conditioned on flood extent data, *Hydrological Processes*, 18, 3347-3370

35 Pappenberger, F., Beven, K.J., Hunter N., Gouweleeuw, B., Bates, P., de Roo, A., Thielen, J., 2005,
36 Cascading model uncertainty from medium range weather forecasts (10 days) through a rainfallrunoff
37 model to flood inundation predictions within the European Flood Forecasting System (EFFS).
38 *Hydrology and Earth System Science*, 9(4), 381-393.

1 Pappenberger, F, Matgen, P, Beven, K J, Henry J-B, Pfister, L and de Fraipont, P, 2006, Influence of
2 uncertain boundary conditions and model structure on flood inundation predictions, *Advances in*
3 *Water Resources*, 29(10), 1430-1449,doi:10.1016/j.advwatres.2005.11.012

4 Pappenberger, F., Beven, K.J., Frodsham, K., Romanowicz, R. and Matgen, P., 2007. Grasping the
5 unavoidable subjectivity in calibration of flood inundation models: a vulnerability weighted approach.
6 *Journal of Hydrology*, 333, 275-287.

7 Romanowicz, R. and Beven, K. J., 2003, Bayesian estimation of flood inundation probabilities as
8 conditioned on event inundation maps, *Water Resources Research*, 39(3), W01073,
9 10.1029/2001WR001056.

10

11 A tidal boundary is mentioned briefly in the site description, however, no further information is
12 provided. Is this boundary condition influential to the model? How was this boundary calculated?

13 R: The astronomical tide (microtidal in nature with tidal range <1 m) is determined using the monthly
14 tidal forecast at a nearby point, published by CICESE (Centro de Investigación Científica y de
15 Educación Superior de Ensenada) for those dates (<http://predmar.cicese.mx/calmen.php>).

16 This information has been included in the manuscript at Page 14 Line 13 – Line 16

1 Propagation of hydro-meteorological uncertainty in a 2 model cascade framework to inundation prediction

3
4 J. P. Rodríguez-Rincón¹, A. Pedrozo-Acuña^{1*} and J. A. Breña-Naranjo¹

5 [1]{National Autonomous University of México, Institute of Engineering, D.F., Mexico}

6 *Correspondence to: A. Pedrozo-Acuña (APedrozoA@ii.unam.mx)

7 8 Abstract

9 ~~The purpose of this~~This investigation ~~is aims~~ to study the propagation of meteorological
10 uncertainty within a cascade modelling approach to flood ~~mapping~~prediction. The methodology
11 was comprised of a Numerical Weather Prediction Model (NWP), a distributed rainfall-runoff
12 model and a ~~standard~~ 2D hydrodynamic model. The ~~cascade~~quantification of ~~models is used to~~
13 ~~reproduce an uncertainty~~ was carried out in a hindcast scenario, removing non-behavioural
14 ensemble members at each stage, based on the fit with observed data. The selected extreme
15 event corresponds to a flood ~~event~~ that took place in the Southeast of Mexico, during November
16 2009. ~~The event was selected as high quality, for which~~ field data (e.g. rain gauges; discharge)
17 and satellite imagery ~~are were~~ available. Uncertainty in the meteorological model (~~Weather~~
18 ~~Research and Forecasting model~~) was ~~evaluated through the use~~estimated by means of a multi-
19 physics ensemble technique, which considers variations in the specific setup options to
20 determine a given precipitation ~~event~~. ~~The resulting precipitation~~. Precipitation fields ~~are~~
21 used from the meteorological model were employed as input in a distributed hydrological
22 model, ~~enabling the determination of different hydrographs associated to this event. Lastly, by~~
23 ~~means of a standard 2D hydrodynamic model, and resulting~~ flood hydrographs ~~are were~~ used as
24 forcing conditions ~~to study in~~ the ~~propagation of the meteorological 2D hydrodynamic model~~.
25 This enabled the assessment of uncertainty ~~to an estimated inundation~~ and its propagation, from
26 a modelled rainfall event to a predicted flooded area. ~~Results show the utility of the selected~~
27 ~~modelling approach to investigate error propagation within a cascade of models and depth.~~
28 Moreover, the evolution of skill within the model cascade shows a complex aggregation of
29 errors between models, suggesting that in valley-filling events hydro-meteorological

1 uncertainty ~~affects~~has a larger effect on inundation depths ~~in a higher degree~~ than that observed
2 in estimated flood inundation extents.

3 4 5 **1 Introduction**

6 Hydro-meteorological hazards can have cascading effects and far-reaching implications on
7 water security, with political, social, economic and environmental consequences. Millions of
8 people worldwide are forcibly displaced as a result of natural disasters, creating political
9 tensions and social needs to support them. These events observed in developed and developing
10 nations alike, highlight the necessity to generate a better understanding on what causes them
11 and how we can better manage and reduce the risk.

12 The assessment of flood risk is an activity that has to be carried out under a framework full of
13 uncertainty. The source of these uncertainties may be ascribed to the involvement of different,
14 and often rather complex models and tools, in the context of environmental conditions that are
15 at best, partially understood ([Hall, 2014](#)). In addition to this, flooding events are dynamic over
16 a range of timescales, due to climate variability and socio-economic changes, among others,
17 which further increases the uncertainty in the projections. Therefore, numerous types of
18 uncertainties can arise when using formal models in the analysis of risks.

19 Uncertainty is often categorised between aleatory and epistemic ([Hacking, 2006](#)): aleatory is
20 an essential, unavoidable unpredictability, and epistemic uncertainty reflects lack of knowledge
21 or the inadequacy of the models to represent reality. In the context of any modelling framework,
22 epistemic uncertainties may be ascribed to the definition of model parameters and to the model
23 structure itself (limited knowledge).

24 In a technological era characterised by the advent of computers, there is an increased ability of
25 more detailed hydrological and hydraulic models. Their use and development has been
26 motivated as they are based on equations that have (more or less) physical justification; and
27 allow a more detailed spatial representation of the processes, parameters and predicted variables
28 ([Beven, 2014](#)). However, there are also disadvantages, these numerical tools take more
29 computer time and require the definition of initial, boundary conditions and parameter values
30 in space and time. Generally, at a level of detail for which such information is not available
31 even in research studies. Moreover, these models may be subjected to numerical problems such

1 as numerical diffusion and instability. All of these disadvantages can be interpreted as sources
2 of uncertainty in the modelling process.

3 Due to wide range of uncertainty sources in the flood risk assessment process, it is of great
4 interest to investigate the propagation and behaviour of these different uncertainties from the
5 start of the modelling framework to the result. The size of registered damages and losses in
6 recent events around the world, reveal the urgency of doing so, even under a context of limited
7 predictability.

8 In September 2013, severe floods were registered in Mexico as a result of the exceptional
9 simultaneous incidence of two tropical storms, culminating in serious damage and widespread
10 persistent flooding (Pedrozo-Acuña et al., 2014a). This unprecedented event is part of a recent
11 set of extreme flood events over the last decade caused by record-breaking precipitation
12 amounts across Central Europe (Becker and Grünwald, 2003), United Kingdom (Slingo et al.,
13 2014), Pakistan (Webster et al., 2011), Australia (Ven den Honert and McAneney, 2011),
14 Northeastern US (WMO, 2011), Japan (WMO, 2011) and Korea (WMO, 2011). In all cases,
15 the immediate action of governments through the implementation of emergency and action
16 plans was required. The main aim of these interventions was to reduce the duration and impact
17 of floods. In addition, risk reduction measures were designed to ensure both a better flood
18 management and an increase in infrastructure resilience.

19 One key piece of information in preventing and reducing losses is given by reliable flood
20 inundation maps that enable the dissemination of flood risk to the society and decision makers
21 (Pedrozo-Acuña et al., 2013). Traditionally, this task requires the estimation of different return
22 periods for discharge (Ward et al., 2011) and their propagation to the floodplain by means of a
23 hydrodynamic model. There is currently a large range of models that can be used to develop
24 flood hazard maps (Horrit and Bates, 2002; Horrit et al., 2006).

25 The aforementioned accelerated progress of computers has given way to the development of
26 model cascades to produce hydrological forecasts, which make use of rainfall predictions from
27 regional climate models (RCMs) with sufficient resolution to capture meteorological events
28 (Bartholomes and Todini, 2005; Demerit et al., 2010). Within this approach, the coupling of
29 different operational numerical models is carried out, using numerical weather prediction
30 (NWP) with radar data for hydrologic forecast purposes (Liguori and Rico-Ramirez, 2012;
31 Liguori et al., 2012), or NWP with hydrological and hydrodynamic models to determine
32 inundation extension (Pappenberger et al., 2012; Cloke et al., 2013; Ushiyama et al., 2014).

1 The use of RCMs in climate impact studies on flooding has been reported by [Teutschbein and](#)
2 [Seibert \(2010\)](#) and [Beven \(2011\)](#), noting that despite their usefulness, the spatial resolution of
3 models (~25km) remains coarse to capture the spatial resolution of precipitation. This is
4 particularly important, as higher resolution is needed to effectively model the hydrological
5 processes essential for determining flood risk. To overcome this limitation, the utilisation of
6 dynamic downscaling in these models has been significantly growing ([Fowler et al., 2007](#);
7 [Leung and Qian, 2009](#); [Lo et al., 2008](#)).

8 Significant challenges remain in the foreseeable future, among these, the inherent uncertainties
9 in the predictive models are likely to have an important role to play. For example, it is well
10 known that the performance skill of NWP's deteriorates very rapidly with time ([Lo et al., 2008](#)).
11 To overcome this, the long-term continuous integration of the prediction has been subdivided
12 into short-simulations, involving the re-initialisation of the model to mitigate the problem of
13 systematic error growth in long integrations ([Giorgi, 1990](#); [Giorgi, 2006](#); [Qian et al., 2003](#)).
14 Moreover, the use of ensemble prediction systems to obtain rainfall predictions for hydrological
15 forecasts at the catchment scale is becoming more common among the hydrological community
16 as they enable the evaluation and quantification of some uncertainties in the results ([Buizza](#)
17 [2008](#); [Cloke and Pappenberger, 2009](#); [Bartholmes et al. 2009](#)). In these studies, an ensemble is
18 a collection of forecasts made from almost, but not quite, identical initial conditions.

19 A key question that arises when using a cascade modelling approach to flood prediction or
20 mapping is: how uncertainties associated to meteorological predictions of precipitation
21 propagate to a given flood inundation map? Previous work has been devoted to the examination
22 of uncertainties in the results derived from different ensemble methods, which address
23 differences in the initial conditions in the NWP or even differences in using a single model
24 ensemble vs. multi-model ensemble ([Pappenberger et al. 2008](#); [Cloke et al., 2013](#); [Ye et al.,](#)
25 [2014](#)). However, less attention has been paid to the behaviour of errors within a model chain
26 that aims to represent a flood event occurring at several spatial scales. In order to understand
27 how errors propagate in a chain of models, this investigation evaluates the transmission of
28 uncertainties from the meteorological model to a given flood map. For this, we utilize a cascade
29 modelling approach comprised by a Numerical Weather Prediction Model (NWP), a rainfall-
30 runoff model and a standard 2D hydrodynamic model. This numerical framework is applied to
31 an observed extreme event registered in Mexico in 2009 for which satellite imagery is available.
32 The investigated uncertainty is limited to the model parameter definition in the NWP model,

1 by means of a multi-physics ensemble technique considering several multi-physics
2 parameterization schemes for the precipitation (Bukovsky and Karoly, 2009). The resulting
3 precipitation fields are used to generate spaghetti plots by means of a distributed hydrological
4 model, enabling the propagation of meteorological uncertainties to the flood hydrograph.
5 Hence, the resulting hydrographs represent the runoff associated to each precipitation field
6 estimated with the NWP. In order to complete the propagation of the uncertainty through the
7 cascade of models to the flood map, the hydrographs are used as forcing in a standard 2D
8 hydrodynamic model.

9 On the other hand, it is acknowledged that each of the other models (hydrological and
10 hydrodynamic) within the model cascade, will introduce other epistemic and random
11 uncertainties to the result. In order to reduce their influence, the numerical setup of both these
12 models is constructed with the best available data (e.g. LiDAR for the topography) and
13 following recent guidelines for the assessment of uncertainty in flood risk mapping (Beven et
14 al. 2011). In this way, the uncertainty associated to the meteorological model outputs is
15 propagated through the model cascade from the atmosphere to the flood plain. Thus, the aim of
16 this investigation is to study the uncertainty propagation from the meteorological model (due
17 to model parameters), to the determination of an affected area impacted by a well-documented
18 hydro-meteorological event.

19 This work is organised as follows: Section 2 provides a description of both, the study area and
20 the extreme hydro-meteorological event, which are employed to test our cascade modelling
21 approach; Section 3 introduces the methodology, incorporating a brief description of the
22 selected models setup. Additionally, we incorporate a description of the multi-physics ensemble
23 technique used to quantify and limit the epistemic uncertainty in the NWP model. The resulting
24 precipitation fields, hydrographs and flood maps are compared with available field data and
25 satellite imagery for the event. In Section 4, a discussion of errors along the model cascade, is
26 also presented with some conclusions and future work.

27

28 **2 Case Study**

29 The selected study area is within the Mexican state of Tabasco, which in recent years has been
30 subjected to severe flooding as reported by Pedrozo-Acuña et al. (2011; 2012). This region
31 comprises the area of Mexico with the highest precipitation rate (2000-3000 mm/year), which
32 mostly occurs during the wet season of the year between May and December. The rainfall

1 climatology is also influenced by the incidence of hurricanes and tropical storms arriving from
2 the North.

3 In this paper, the extreme hydro-meteorological event selected for the analysis corresponds to
4 that registered in the early days of November 2009 in the Tonalá river. As it is shown in Fig.1,
5 the river is located in the border of Tabasco and Veracruz and during the event, the substantial
6 rainfall intensity provoked its overflowing leaving extensive inundated areas along its
7 floodplain. Top panel of Fig. 1 shows the geographical location of the catchment, with an area
8 of 5,021 km², as well as the location of 18 weather stations installed within the region by the
9 National Weather Service. The event was the result of heavy rain induced by the cold front #9,
10 which persisted for four days along Mexico's Gulf Coast, forcing more than 44,000 people to
11 evacuate their homes and affecting more than 90 communities. High intensities in rainfall were
12 recorded in rain gauges from the 31st October to 3rd November, with cumulative daily
13 precipitation values reporting more than 270 mm. The river is approximately 300 km long and
14 before discharging into the Gulf of Mexico, the stream receives additional streamflow from
15 other smaller streams such as Agua Dulcita in Veracruz, and Chicozapote in Tabasco. The
16 bottom panel of the same Figure illustrates the lower Tonalá River, where severe flooding was
17 registered as it is shown in the photographs on the right. The yellow, blue and red dots on the
18 panel represent the location at which the photographs were taken.

19 The hydrometric data in combination with the satellite imagery for the characterisation of the
20 affected areas, enabled an accurate investigation of the causes and consequences that generated
21 this flood event. The high quality of the available information, allowed the application of a
22 cascade modelling approach comprised by state-of-the-art meteorological, hydrological and
23 hydrodynamic models. This numerical approach is utilised with the intention to carry out an
24 assessment of the modelling framework, with particular emphasis on the propagation of the
25 epistemic uncertainty from the meteorological model to the spatial extent of an affected area.
26 Such investigation paves the road towards a more honest knowledge transfer to decision-
27 makers, whom consider the reliability of the model results.

28

29 **3 Methodology and Results**

30 The methodology is comprised of a Numerical Weather Prediction Model (NWP), a distributed
31 rainfall-runoff model and a standard 2D hydrodynamic model. It is anticipated that the selected
32 modelling approach will support the advance of the understanding of the connections among

1 scales, intensities, causative factors, and impacts of extremes. This model cascade with state-
2 of-the-art numerical tools representing a hydrological system, enables the development of a
3 framework by which an identification of the reliability of simulations can be undertaken. This
4 framework is utilised to explore the propagation of epistemic uncertainties from the estimation
5 of precipitation in the atmosphere to the identification of a flooded area. Therefore, the aim is
6 not to reproduce an observed extreme event, but to investigate the effects of errors in rainfall
7 prediction by a NWP on inundation areas.

8 The proposed investigation is important as uncertainties are cascaded through the modelling
9 framework, in order to provide better understanding on how errors propagate within models
10 working at different temporal and spatial scales. It is acknowledged that this information would
11 enhance better flood management strategies, which would be based on the honest and
12 transparent communication of the results produced by a modelling system constrained by
13 intrinsic errors and uncertainties.

14

15 **3.1 Meteorological model**

16 Simulated precipitation products from numerical weather prediction systems (NWPs) typically
17 show differences in their spatial and temporal distribution. These differences can considerably
18 influence the ability to predict hydrological responses. In this sense, in this study we utilise the
19 advanced research core of the Weather Research and Forecasting (WRF) model Version 3.2.
20 The WRF model is a fully compressible non-hydrostatic, primitive-equation model with
21 multiple nesting capabilities ([Skamarock et al., 2008](#)).

22 As it is shown in [Fig. 2](#), the model setup is defined using an interactive nested domain inside
23 the parent domain. This domain is selected in order to simulate more realistic rainfall, with the
24 inner frame enclosing the Tonalá river catchment within a 4 km resolution. The 4 km horizontal
25 resolution is considered good enough to compute a mesoscale cloud system associated to a cold
26 front. It is shown that this finer grid covers the central region of Mexico, while in the vertical
27 dimension, 28 unevenly spaced sigma levels were selected. The initial and boundary conditions
28 were created from the NCEP Global Final Analysis (FNL) with a time interval of 6 hours for
29 the initial and boundary conditions. Each of the model simulations was reinitialised every two
30 days at 1200 UTC, considering a total simulation time from the 27th October 2009 until the 13th
31 November 2009.

1 Epistemic uncertainty is considered in the WRF model by means of the sensitivity of the results
2 for precipitation, due to variations in the model setup. For this, we utilise a multi-physics
3 ensemble technique proposed by Bukovsky and Karoly (2009), where the sensitivity of
4 simulated precipitation in the model results is examined through variations in the specific setup
5 options by means of twenty three different combinations. The comparison of computed
6 precipitation fields against real measurements from weather stations within the catchment,
7 enabled the quantification of uncertainty in the meteorological model for this event. **Table 1**
8 shows a summary of the different multi-physics parameters used in the WRF model to generate
9 the physics ensemble. As it is shown on this table, there is a large discrepancy in the model skill
10 results in all 23 simulations Error metrics reported in this table are computed using information
11 from all available stations within the numerical domain; which comprised stations that are
12 outside the area of the catchment. It is demonstrated that only 13 of these model runs report a
13 positive Nash-Sutcliff Coefficient (NSC), which indicates a better accuracy for those
14 realisations. In contrast, model runs with negative NSC were dismissed for the numerical
15 reproduction of the event, as this condition is a clear indicator that the observed mean is a better
16 predictor than the model.

17 Therefore, meteorological model runs that comply with a criteria defined by a $NSC > 0.3$ and a
18 Correlation coefficient ($Cor > 0.8$) (for the whole numerical domain) are utilised to investigate
19 the propagation of meteorological uncertainties through the modelling framework. This criteria
20 narrows down the meteorological model runs to 12, which will be cascaded to the hydrological
21 model stage to attain streamflow predictions. In this approach, the selected 12 multi-physics
22 ensemble runs of the model represent a plausible and equally likely state of the system in the
23 future.

24 **Fig. 3** illustrates the cumulative precipitation curves computed for each of the 23 model runs of
25 the multi-physics ensemble at four different stations located within the catchment. In this figure
26 differences in the spatial distribution and intensity of precipitation are evident. Moreover, the
27 selected 12 members by the criteria ($NSC > 0.3$ and $Cor > 0.8$) are illustrated by the blue solid
28 lines, while the grey solid lines show those members that were rejected by it. Notably,
29 dismissed members tend to underestimate the amount of precipitation in all four locations that
30 are presented in this figure. For completeness, the rainfall measurements at each meteorological
31 station are also shown by the black solid line, while the red dotted line depicts the mean value
32 of the selected model runs to be propagated through the model cascade. If the 12 selected

1 members are considered in the estimation of ensemble metrics at each station, it is shown that
2 at Station No. 27075, the spread of the estimated cumulative precipitation curves is limited and
3 quantified by a NSC=0.917 and a NRMSE = 10.7%, indicating a good skill of the selected WRF
4 precipitation estimates at this point. In contrast, at Station No. 27007 the spread of the
5 cumulative precipitation is large and characterised by a NSC=0.766 and a NRMSE=19.4%,
6 showing less skill in the model performance than that observed in the previous case. The
7 observed differences of estimated precipitation for this event, highlight the importance of
8 incorporating ensemble techniques in the reproduction of precipitation with this type of models.

9 **Fig. 4** illustrates the cumulative precipitation fields computed for each of the 12 selected
10 members of the multi-physics ensemble, where differences in the spatial distribution and
11 intensity of precipitation were evident. These results suggest that for this event, the precipitation
12 field estimated with the WRF was highly sensitive to the selection of multi-physics parameters.
13 To revise in more detail the performance of the WRF in reproducing this hydro-meteorological
14 event, the estimated cumulative precipitation by each of the selected 12 members of the multi-
15 physics ensemble was compared against measurements at the eighteen weather stations located
16 within and close to the Tonalá catchment.

17 **Table 2** presents a summary of the most well-known error metrics calculated at each weather
18 station and for each member of the ensemble. Among these are the: Normalised Root-Mean
19 Square Error (NRMSE), BIAS, Nash-Sutcliffe Coefficient (NSC), and the Correlation
20 coefficient (Cor). The columns show the local value of each coefficient for a given member of
21 the ensemble (M1, ..., M12). As shown in all columns (i.e. member runs), the error metrics
22 have a great spatial variability, hence, indicating the regions of the study area where the model
23 performs better. To illustrate the performance of this ensemble technique at each weather
24 station, the ensemble average of these error metrics is introduced in the last column and
25 indicated by < >. Again, the spatial variability of the metrics is evident. The two bottom rows
26 in each sub-table correspond to the average of the ensemble averages for the whole catchment
27 and for the all the stations. It is shown, that when the average of all stations is taken into account,
28 the skill decreases. However, in this investigation the error that is of interest is the one
29 corresponding to the average of those weather stations located within the catchment, as these
30 will be used as input in the hydrological model. This will enable the propagation of errors in
31 the meteorological model within the model cascade. For clarity, in the same table the stations
32 within the catchment are highlighted in blue.

1 A question that has been seldom explored in the literature, is how the uncertainty in the
2 prediction of the precipitation (i.e. errors described in this section), cascade into an estimated
3 flood hydrograph determined by a distributed hydrological model. In this sense, the next step
4 in this work, considers the non-linear transfer of rainfall to runoff using a distributed rainfall-
5 runoff model. For this, we employ each one of the selected 12 precipitation fields derived from
6 the WRF as input to determine the associated river discharge with the hydrological model.

7

8 **3.2 Hydrological model**

9 The hydrological model used in this study was applied to the Tonalá River catchment in an
10 early work presented by [Rodríguez-Rincón et al. \(2012\)](#). This numerical tool was developed by
11 the Institute of Engineering – UNAM ([Domínguez-Mora et al., 2008](#)), and comprises a
12 simplified grid-based distributed rainfall–runoff model. The model has been previously applied
13 with success in other catchments in Mexico (e.g. [Pedrozo-Acuña et al., 2014b](#)).

14 The model is based on the method of the Soil Conservation Service (SCS) with a modification
15 that allows the consideration of soil moisture accounting before and after rainfall events. The
16 parameters that are needed for the definition of a runoff curve number within the catchment are
17 the hydrological soil group, land use, pedology and the river drainage network. [Fig. 5](#) shows
18 for the Tonalá River catchment, the spatial definition of the river network (center panels) and
19 the runoff curve (right panels). For the numerical setup of the hydrological model, we employ
20 topographic information from a LiDAR data set, from which a 10m resolution Digital Elevation
21 Model (DEM) is constructed.

22 There are two main hypothesis that underpin the SCS curve number method. Firstly, it is
23 assumed that for a single storm and after the start of the runoff, the ratio between actual soil
24 retention and its maximum retention potential is equal to the ratio between direct runoff and
25 available rainfall. Secondly, the initial infiltration is hypothesised to be a fraction of the
26 retention potential.

27 Thus, the water balance equation and corresponding assumptions are expressed as follows:

$$28 \quad P = P_e + I_a + F_a \quad (1)$$

$$29 \quad \frac{P_e}{P_a - I_a} = \frac{F_a}{S} \quad (2)$$

30

$$1 \quad I_a = \lambda S \quad (3)$$

2 Where P is rainfall, P_e effective rainfall, I_a is the initial abstraction, F_a is the cumulative
 3 abstraction, S is the potential maximum soil moisture retention after the start of the runoff and
 4 λ is the scale factor of initial loss. The value of λ is related to the maximum potential infiltration
 5 in the basin.

6 Through the combination of equations (1) - (3) and expressing the initial abstraction (I_a) by
 7 $0.2*S$ we have:

$$8 \quad P_e = \frac{(P - 0.2S)^2}{P + 0.8S} \quad (4)$$

10 where, the value of S [cm] is determined by:

$$11 \quad S = \frac{2450 - (25.4CN)}{CN} \quad (5)$$

13 CN is the runoff curve number, as defined by the Agriculture Department of the USA ([USDA,](#)
 14 [1985](#)). Values for this parameter vary from 30 to 100, where small numbers indicate low runoff
 15 potential while larger numbers indicate an increase in runoff potential. Thus, the permeability
 16 of the soil is inversely proportional to the selected curve number. Another parameter that allows
 17 the modification of the curve number is the soil water potential given by F_s , following $S = S * F_s$.

18 The model includes a parameter to reproduce the effects of evaporation on the ground saturation
 19 (F_o). This parameter is useful when the event to be reproduced lasts for several days; however,
 20 due to the duration of this event it is assumed equal to 0.9 in all cases. The computation of the
 21 runoff in the basin is carried out through the addition of the runoff estimated in each cell to then
 22 construct a general hydrograph (See [Rodríguez-Rincón et al. 2012](#)). With regards to the
 23 definition of values for the other two free parameters in the hydrological model (λ and F_s), a
 24 traditional calibration process is implemented. For this, we utilise flood hydrographs from past
 25 extreme events (2001, 2005, 2007, 2008, 2009 and 2011) observed in this river. For these
 26 events, we employ as rainfall input the registered precipitation at the same 4 weather stations
 27 that are within the river catchment, which location is shown in the top panel of **Figure 1**.

28 Therefore, we determine six sets of free parameters that are good enough to represent the
 29 rainfall-runoff relationship in this catchment. The selected sets of values are illustrated in **Table**
 30 **3**, where the correlation coefficient and NSC are also reported for each of the years. It is shown

1 that in all the events, the selected set of parameters ensures a good correlation against the
2 observed discharge which is given by $Cor > 0.7$, as well as a positive NSC (accuracy).

3 It is well known that both the amount and distribution of rainfall can significantly affect the
4 final estimated river discharge (Ferraris et al. 2002; De Roo et al., 2003; Cluckie et al., 2004).
5 In consequence, the propagation of meteorological uncertainty to the rainfall-runoff model is
6 carried out using the 12 WRF rainfall precipitation ensembles as an input in the hydrological
7 model, considering the six sets of free parameters reported in **Table 3**. This procedure enabled
8 the generation of 72 hydrographs that could represent the 2009 event with different skill. Error
9 metrics of all the computed hydrographs are reported in **Table 4**.

10 For completeness, **Fig. 6a** illustrates the 72 computed hydrographs for the Tonalá River
11 catchment in relation to the measured river discharge for the 2009 event (blue dashed line). It
12 is shown that if all 72 hydrographs are taken into account, uncertainty bounds are significant.
13 Indeed, this illustrates the interaction of the meteorological uncertainty with that coming from
14 the setup of the hydrological model (definition of free parameters). However, the purpose of
15 this study is to investigate in a model cascade framework, how errors in the meteorological
16 prediction stage propagate down to a predicted inundation. In this sense, we narrow down the
17 number of hydrographs shown in **Fig. 6a**, by selecting only those with a $Cor > 0.7$ and $NSC > 0.6$,
18 as reported in **Table 4** only 31 out of 72 (shown in bold) follow this condition. **Fig. 6b** displays
19 the 31 selected hydrographs along with the measured discharge for the 2009 event. Although
20 there is a reduction in the uncertainty bounds, it is shown that errors in the predicted rainfall
21 are indeed propagated to the hydrological model, which employs a finer spatial resolution (1
22 km). It has been established that, in some cases, an error in the meteorological model can be
23 compensated by an error in the hydrological model and vice-versa. To illustrate this in more
24 detail, average values of the calculated error metrics for the 31 selected hydrographs are
25 estimated and reported in **Table 4**, with $NSC = 0.79$, $Cor = 0.96$ and $BIAS = 1.11$. Values of the
26 NSC for selected hydrographs in **Table 4** illustrate the resulting differences in skill resulting
27 from the combination of different setups in the hydrological model with the multi-physics
28 ensemble. For instance, in the rows corresponding to the parameters determined for the 2011
29 event, member M12 indicates a $NSC = 0.738$ showing a poorer skill at reproducing the river
30 discharge with the precipitation derived from this member, in comparison to that registered for
31 member M2 with $NSC = 0.938$. The change in the values of the NSC indicates that results from

1 the regional weather model can be enhanced or weakened by the performance of the
2 hydrological model.

3 The utilisation of the 31 selected hydrographs in a 2D hydrodynamic model enables the study
4 of the propagation of errors within the cascade of models. In particular, for estimating the flood
5 extent during this extreme event.

6

7 **3.3 Flood inundation model**

8 Several 2D hydrodynamic models have been developed for simulating extreme flood events.
9 However, any model is only as good as the data used to parameterise, calibrate and validate the
10 model. 2D models have been regarded as suitable for simulating problems where inundation
11 extent changes dynamically through time as they can easily represent moving boundary effects
12 (e.g. [Bates and Horritt, 2005](#)). The use of these numerical tools has become common place
13 when flows produce a large areal extent, compared to their depth and where there are large
14 lateral variations in the velocity field ([Hunter et al., 2008](#)).

15 In this study, given the size of the study area the modelling system utilised is comprised by the
16 flow model of MIKE 21 flexible mesh (FM). This numerical model solves the two dimensional
17 Reynolds-averaged Navier–Stokes equations invoking the approximations of Boussinesq and
18 hydrostatic pressure (for details see [DHI, 2014](#)). The equations are solved at the centre of each
19 element in the model domain.

20 The numerical setup is based on a previous work on the study area ([Pedrozo-Acuña et al. 2012](#)),
21 with selected resolutions for the elements of the mesh with a size that guarantees the proper
22 assimilation of a 10 m DEM to characterise the elevation in the floodplain. The topographic
23 data has been regarded as the most important factor in determining water surface elevations,
24 base flood elevation, and the extent of flooding and, thus, the accuracy of flood maps in riverine
25 areas ([NRC, 2009](#)). Therefore, the elevation data used in this study corresponds to LiDAR data
26 set provided by [INEGI \(2008\)](#). The choice of a 10-m DEM is based on recommendations put
27 forward by the Committee on Floodplain Mapping Technologies, [NRC \(2007\)](#) and [Prinos et al.](#)
28 [\(2008\)](#), as such a DEM ensures both accuracy and detail of the ground surface. The model
29 domain is illustrated in [Fig. 7](#), along with the numerical mesh and elevation data, it comprises
30 the lower basin of the Tonalá River and additional main water bodies. The colours represent
31 the magnitude of the elevation and bathymetric data assimilated in the numerical mesh, where

1 warm colours identify high ground areas and light blues represent bathymetric data. The
2 integration of high quality topographic information in a 2D model with enough spatial
3 resolution, enables the investigation of the propagation of the meteorological uncertainty to the
4 determination of the flood extent. Moreover, as it is illustrated in **Fig. 7** the numerical mesh
5 considers three boundary conditions. These are input flow boundary where the hydrograph from
6 the rainfall-runoff model is set (red dot); the Tonalá's river mouth, where the astronomical tide
7 occurs for the period of the event (27th October – 12th November 2009) (yellow dot) and the
8 Agua Dulcita river set where a constant discharge of 100 m³/s is introduced (blue dot). The
9 astronomical tide (microtidal in nature with tidal range <1 m) is determined using the monthly
10 tidal forecast at a nearby point, which is published by CICESE (Centro de Investigación
11 Científica y de Educación Superior de Ensenada) and it is available at
12 (<http://predmar.cicese.mx/calmen.php>).

13 On the other hand, hydraulic roughness is a lumped term known as Manning's coefficient that
14 represents the sum of a number of effects, among which are skin friction, form drag and the
15 impact of acceleration and deceleration of the flow. The precise effects represented by the
16 friction coefficient for a particular model depend on the model's dimensionality, as the
17 parameterisation compensates for energy losses due to unrepresented processes, and the grid
18 resolution (Bates et al., 2014). The lack of a comprehensive theory of "effective roughness"
19 have determined the need for calibration of friction parameters in hydraulic models.
20 Furthermore, the determination of realistic spatial distributions of friction across a floodplain
21 in other studies, have showed that only 1 or 2 floodplain roughness classes are required to match
22 current data sources (Werner et al., 2005). Indeed, this suggests that application of complex
23 formulae to establish roughness values for changed floodplain land use are inappropriate until
24 model validation data are improved significantly. Therefore, in this study hydraulic roughness
25 in the floodplain is assumed to be uniform and different from the main river channel, in this
26 sense two values for the Manning number are used, one for the main river channel ($M=32 \text{ m}^{1/2}\text{s}^{-1}$)
27 and another for the floodplain ($M=28 \text{ m}^{1/2}\text{s}^{-1}$).

28 It should be noted that several investigations confirm that there is significant uncertainty
29 associated with flood extent predictions using hydraulic models (e.g. Aronica et al., 1998, 2002;
30 Bates et al. 2004; Pappenberger et al., 2005, 2006, 2007; Romanowicz and Beven, 2003). These
31 uncertainties may be ascribed to differences in spatio-temporal resolutions or the hydraulic
32 roughness that is used in the hydraulic model. In this investigation, however, a more detailed

analysis of the different sources of uncertainty in the hydraulic model is not implemented. The numerical setup of the hydraulic model is built following published guidelines for an accurate representation of the case study (see Asselman et al. 2008), which enables us to build the discussion on how an uncertainty generated at the meteorological stage of the model chain propagates and influences a resulting flooded area and depth.

In order to assess whether the 2D model is able to reproduce the flood extent observed in 2009, numerical results of flood extent are compared against the affected area determined from a SPOT image (resolution of 124m). This practice is widely used in the literature to evaluate the results from inundation models and to compare its performance (Di Baldassare et al, 2010b; Wright et al., 2008).

Fig. 8a introduces the result of the hydrodynamic simulation for each of the 31 selected hydrographs, which resulted from the utilisation of the rainfall-runoff model using as input the WRF multi-physics ensemble output. The illustrated flood map summarises the 31 different possibilities of the inundation area that could result from the characterisation of precipitation with the WRF model. Each of these flood maps can also be associated to a probability enabling the representation of a probabilistic flood map, shown in the figure. This allows the identification of the areas highly vulnerable to flooding from this event. Additionally, **Fig. 8b** introduces the infrared SPOT satellite image of the 12th of November 2009, which is used for comparison against the produced flood maps derived from running the 31 hydrographs as inputs in the 2D model. Notably, in the numerical results, the blue area identifies the region of the domain that is most likely to be flooded (90%), the comparison of this area with the observed inundation in the satellite image, show a good skill of the model chain at reproducing the registered flood in the study area.

Despite the variability in the estimated peak discharge utilised as input in the different hydrodynamic runs, inundation results show similar affected areas in all realisations (only with small differences in its size). This is verified in the results shown in **Fig. 9a**, where the relationship between peak discharge of the 31 hydrographs, is plotted against the size of the maximum-flooded area. The distribution of points in this graph clearly indicates that although there are differences in the estimated peak flow (see histogram in **Fig. 9b**), in most cases the resulting size of the inundated area is similar. Histogram plot shown in **Fig. 9c** indicates a clear concentration numerically derived flooded areas with a size larger than 130 km². Indeed, the

1 mean value of the maximum-flooded estimated area is 138.94 km², while the standard deviation
2 is 16.09 km².

3 These results support that the hydraulic behaviour in all hydrodynamic simulations was indeed
4 very similar, regardless of the peak discharge of the hydrograph. It is reflected that this may be
5 the result of induced hydrodynamics by a valley-filling flood event, which is identified with the
6 relatively high floodplain area-to-channel-depth ratios in all simulations. Hence, all possible
7 hydrographs generated with the hydrological model show similar levels of lateral momentum
8 exchange between main channel and floodplain. For this reason, the predictive performance of
9 all hydrodynamic simulations used to reproduce the inundation extent appears to be good (see
10 **Table 5**).

11 The estimation of several error metrics in these results was performed using binary flood extent
12 maps, where the comparison is based on the generation of a contingency table, which reports
13 the number of pixels correctly predicted as wet or dry. From this, measures of fit such as: BIAS,
14 False Alarm Ratio (FAR), Probability of Detection (POD), Probability of False Detection
15 (POFD), Critical Success Index (CSI) and the True Skill Statistics (TSS) are estimated. **Table**
16 **5** introduces the results for all 31 members and error metrics. Clearly, there is little variability
17 in the performance of the model for each of the runs, showing that there has been a small
18 propagation of the error to the flood map. The ensemble average of these quantities is also
19 illustrated in the last column of the table, where values of BIAS=1.013, FAR=0.189,
20 POD=0.819, POFD=0.180; CSI=0.686 and TSS=0.639 are reported. As noted before, these
21 results indicate an apparent good skill of the model chain at reproducing the flood extension,
22 due to the incidence of this extreme event. It should be borne in mind, however, that some
23 misclassification errors may also be included in the observed flooded area due to specular
24 reflections that may classify some wet vegetation as water or open water as dry land. In
25 consequence, flood extent maps should be used with caution in assessing model performance
26 ([Di Baldassare, 2012](#)). This is particularly true during high-magnitude events where the valley
27 is entirely inundated, such as the case study of this investigation where small changes in lateral
28 flood extent may produce large changes in water levels.

29 In this sense, it has been argued that flood extent maps are not useful for model assessment
30 ([Hunter et al., 2005](#)) and high water marks are more useful to evaluate model performance.
31 Unfortunately, for the case study information of inundation depths was not available. Despite
32 this fact, a further revision of simulated inundation depths is also carried out. For this, 10 points

1 distributed within the numerical domain are selected. These are illustrated by the coloured dots
2 in [Fig. 10](#), along with the values of mean water depth in all the 31 simulations (red solid line).
3 In all cases, a high variability in the estimated inundation depth on the floodplain is depicted
4 (with values varying between 1.5 and 3m). This result supports that in the case of valley-filling
5 flood events, there is a higher sensitivity to errors in the vertical dimension of the flood.

6 In one hand, this demonstrates that the geomorphological characteristics of the site (e.g. low-
7 lying area, smooth slopes in the river channel and floodplain) are dominant in the accurate
8 determination of the magnitude of an inundated area, regardless of the peak discharge. This
9 implies that for this type of rivers and when predicting inundation extent, it may be more
10 important to have a good characterisation of the river and floodplain (e.g. high quality field data
11 and a LiDAR derived DEM), than a good characterisation of the rainfall-runoff relationship.

12 Current approaches to flood mapping, have pointed out that in order to produce a scientifically
13 justifiable flood map, the most physically-realistic model should be utilised ([Di Baldassarre et
14 al., 2010](#)). Nevertheless, even with these models the amount of uncertainty involved in the
15 determination of an affected area is important and should be quantified.

16

17 **4 Discussion and Conclusions**

18 Flood risk mapping and assessment are highly difficult tasks due to the inherent complexity of
19 the relevant processes, which occur in several spatial and temporal scales. As pointed out by
20 [Aronica et al. \(2013\)](#), the processes are subject to substantial uncertainties (epistemic and
21 random), which emerge from different sources and assumptions, from the statistical analysis of
22 extreme events and from the resolution and accuracy of the DEM used in a flood inundation
23 model.

24 By acknowledging that all models are an imperfect representation of the reality, it is important
25 to quantify the impact of epistemic uncertainties on a given result. The numerical approach
26 utilised in this investigation enabled an assessment of a state-of-the art modelling framework,
27 comprised by meteorological, hydrological and hydrodynamic models. Emphasis was given to
28 the effects of epistemic uncertainty propagation from the meteorological model to the definition
29 of an affected area in a 2D domain. Ensemble climate simulations have become a common
30 practice in order to provide a metric of the uncertainty associated with climate predictions. In
31 this study, a multi-physics ensemble technique is utilised to evaluate the propagation of

1 epistemic uncertainties within a model chain. Therefore, the assessment of hydro-
2 meteorological model performance at the three stages is carried out through the estimation of
3 skill scores.

4 **Fig. 11** presents a summary of the propagation of two well-known error metrics, BIAS (top
5 panel) and NSC/TSS (bottom panel). These metrics were selected, as they enable a direct
6 comparison of their values at each of the stages within the model cascade. In both metrics, the
7 evolution of the confidence limits is illustrated by the size of the bars. Their evolution from the
8 meteorological model to the hydrological model, show an aggregation of meteorological
9 uncertainties with those originated from the rainfall-runoff model. However, the skill is
10 considerably improved from a mean value of 0.65 in the meteorological model, to 0.793 in the
11 hydrological model. In the last stage of the model chain (hydrodynamic model), the confidence
12 limits of the results, show an apparent improvement in model skill. However, it should be noted
13 that this may be ascribed to the complex aggregation of errors in valley-filling events, which is
14 verified in the observed sensitivity of the simulated inundation depths. The mean value of the
15 skill is reduced to TSS=0.639. The results provide an useful way to evaluate the hydro-
16 meteorological uncertainty propagation within the modelling cascade system.

17 BIAS and NSC/TSS error metrics (**Fig. 11**) revealed discrepancies between observations and
18 simulations throughout the model cascade. For instance, an increase in the NSC from the
19 rainfall to the flood hydrograph it implies that the hydrological model is more sensitive (wider
20 uncertainty bars) to its main input (precipitation) than the WRF model is to the set of micro-
21 physics parameterisations. On the other side, the uncertainty bounds in the hydrological model
22 imply a high sensitivity of hydrographs to both, errors from the meteorological model and its
23 numerical setup with free parameters (amplifying the uncertainty). This is observed in the
24 spaghetti plot shown in **Fig. 6a**, where large uncertainty bounds were identified. In order to
25 reduce errors from the interaction of uncertainties coming from both models, these bounds were
26 reduced with the selection of 31 hydrographs that comply with $Cor > 0.7$ and $NSC > 0.6$ (see
27 **Fig.6b**). It is reflected that the estimated error in the meteorological model may reflect a spatial
28 scaling issue (comparing observations from rain gauges to simulations at the meso-scale).

29 Results concerning predictions of inundation extent indicate an apparent good skill of the model
30 chain at reproducing the flood extension. The propagation of uncertainty and error from the
31 hydrological model to the inundation area revealed that is necessary to assess model
32 performance not only for flood extension purposes, but also to estimate inundation depths,

1 where results indicate a higher variability (e.g. increase in the error). This last modelling step
2 is quite important given the consequences for issuing warning alerts to the population at risk.

3 The similar magnitude in inundation extents of all numerical results indicated the predominance
4 of a valley-filling flood event, which was characterised by a flooded area strongly insensitive
5 to the input flood hydrograph. While this can be explained by the limited effect that the volume
6 overflowing the riverbanks and reaching the floodplain will have on the maximum inundation
7 area, the difference between the observed and the simulated flooded area remains important
8 (TSS=0.639).

9 It should be pointed out, that this methodology contains more uncertainties that were not
10 considered or quantified in the generation of flood extent maps for this event. To quantify the
11 epistemic uncertainty in the larger scale (i.e. atmosphere), a mesoscale numerical weather
12 prediction system was used along with a multi-physics ensemble. The ensemble was designed
13 to represent our limited knowledge of the processes generating precipitation in the lower
14 troposphere. It was shown that a large amount of uncertainty exists in the NWP model, and
15 such uncertainty is indeed propagated over the catchment and floodplain. Members of the
16 ensemble were shown to differ significantly in terms of their cumulative precipitation, spatial
17 distribution, river discharge, inundation depths and areas. Therefore, epistemic uncertainties
18 from each step in this model cascade can be aggregated up to the final output.

19 The evaluation of the skill in the model cascade shows further potential for improvements of
20 the modelling system. Consequently, future work is planned to include the remaining
21 uncertainties as adopted by, e.g. [Pedrozo-Acuña et al. \(2013\)](#). Special attention should be paid
22 to the interaction between hydro-meteorological and hydrological uncertainty, as well as flood
23 extent estimation in catchments with different morphological setting. The assessment of the
24 error propagation within the model cascade is seen as a good step forward, in the
25 communication of uncertain results to the society. However, as shown in this work, an
26 improvement in model prediction during the first cascade step (rainfall to runoff) can be
27 reverted during the second cascade step (runoff to inundation area) with important
28 consequences for early warning systems and operational forecasting purposes. Finally, the
29 proposed numerical framework could be utilised as a robust alternative for the characterisation
30 of extreme events in ungauged basins.

31

32 **Acknowledgements**

1 The authors thank the financial support from the Institute of Engineering, UNAM, through
2 internal and international grants. The authors gratefully acknowledge the comments and
3 suggestions made by two anonymous referees and Prof. Jim Freer, handling editor of this
4 manuscript.

5

6 **References**

7 Aronica, G. T., Apel, H., Baldassarre, G. D. and Schumann, G. J.-P. 2013. HP – Special Issue
8 on Flood Risk and Uncertainty. *Hydrol. Process.*, 27: 1291. doi: 10.1002/hyp.9812

9 [Aronica, G, Hankin, B.G., Beven, K.J., 1998, Uncertainty and equifinality in calibrating](#)
10 [distributed roughness coefficients in a flood propagation model with limited data, *Advances in*](#)
11 [*Water Resources*, 22\(4\), 349-365](#)

12 [Aronica, G., Bates, P.D. and Horritt, M.S., 2002. Assessing the uncertainty in distributed model](#)
13 [predictions using observed binary pattern information within GLUE. *Hydrological Processes*,](#)
14 [16, 2001- 2016.](#)

15 [Asselman, N., Bates P., Woodhead S., Fewtrell T., Soares-Frazaõ S., Zech Y., Velickovic M.,](#)
16 [de Wit A., ter Maat J., Verhoeven G., Lhomme J. 2008. Flood Inundation Modelling – Model](#)
17 [Choice and Proper Application, Report T08-09-03, FLOODsite Project.](#)

18 Bartholmes, J., Todini, E. 2005. Coupling meteorological and hydrological models for flood
19 forecasting, *Hydrol. Earth Syst. Sci.*, 9, 333-346, doi:10.5194/hess-9-333-2005.

20 Bartholmes, J., Thielen, J., Ramos, M., Gentilini, S., 2009. The European flood alert system
21 EFAS – Part 2: statistical skill assessment of probabilistic and deterministic operational
22 forecasts. *Hydrology and Earth System Sciences*, 2: 141–153.

23 [Bates, P. D., Horritt, M. S., Aronica, G. and Beven, K J, 2004, Bayesian updating of flood](#)
24 [inundation likelihoods conditioned on flood extent data, *Hydrological Processes*, 18, 3347-3370](#)

25 Bates, P.D., Horritt, M.S. 2005. Modelling wetting and drying processes in hydraulic models.
26 In Bates, P.D., Lane, S.N. and Ferguson, R.I. (eds), *Computational Fluid Dynamics:*
27 *applications in environmental Hydraulics*, John Wiley and Sons, Chichester, UK

28 Bates, P.D., Pappenberger, F., Romanowicz, R.J. 2014. Uncertainty in Flood Inundation
29 Modelling. In Beven, K.J., and Hall, J. (eds.), *Applied Uncertainty Analysis for Flood Risk*
30 *Management*, Imperial College Press, World Scientific, London, UK

- 1 Becker, A. & Grünewald, U. 2003. Flood risk in central Europe. *Science* 300, 1099.
- 2 Beven, K.J. 2011. I believe in climate change but how precautionary do we need to be in
3 planning for the future? *Hydrological Processes* 25: 1517–1520.
- 4 Beven, K.J. 2014. Use of Models in Flood Risk Management. In Beven, K.J., and Hall, J. (eds.),
5 Applied Uncertainty Analysis for Flood Risk Management, Imperial College Press, World
6 Scientific, London, UK
- 7 Beven, K., Leedal, D., McCarthy, S., Lamb, R., Hunter, N., Keef, C., Bates, P., Neal, J. and
8 Wicks, J. 2011. Framework for Assessing Uncertainty in Fluvial Flood Risk Mapping. FRMRC
9 Research Report SWP1.7
- 10 Buizza R. 2008. The value of probabilistic prediction. *Atmospheric Science Letters*, 9: 36–42.
- 11 Bukovsky, M. S. and D. J. Karoly. 2009. Precipitation simulations using WRF as a nested
12 regional climate model. *Journal of Applied Meteorology and Climatology*, 48(10): 2152-2159.
- 13 Cloke, H. L. and Pappenberger, F. (2008). Evaluating forecasts for extreme events for
14 hydrological applications: an approach for screening unfamiliar performance measures,
15 *Meteorol. Appl.*, 15(1), 181–197.
- 16 Cloke, H.L., Pappenberger, F. 2009. Ensemble flood forecasting: A review. *Journal of*
17 *Hydrology*, doi:10.1016/j.jhydrol.2009.06.005
- 18 Cloke, H. L., Wetterhall, F., He, Y., Freer, J. E. and Pappenberger, F. 2013. Modelling climate
19 impact on floods with ensemble climate projections. *Q.J.R. Meteorol. Soc.*, 139: 282–297. doi:
20 10.1002/qj.1998
- 21 Cluckie I., Han D., Xuan Y. 2004. Preliminary Analysis on NWP-Based QPF over UK domain.
22 Deliverable 4.2, FLOODRELIEF Project, URL: <http://projects.dhi.dk/floodrelief/>
- 23 Committee on Floodplain Mapping Technologies, NRC. 2007. Elevation data for floodplain
24 mapping. Washington, DC: National Academic Press.
- 25 Committee on FEMA Flood Maps; Board on Earth Sciences and Resources/Mapping Science
26 Committee; NRC. 2009. Mapping the Zone: Improving Flood Map Accuracy. Washington, DC:
27 National Academic Press.
- 28 CONAGUA. *Atlas digital del Agua México 2010*, Sistema Nacional de Información del Agua
29 (2010). <ftp://ftp.conagua.gob.mx/>.

1 Cuo, L., T. C. Pagano, and Q. J. Wang, 2011: A review of quantitative precipitation forecasts
2 and their use in short to medium range streamflow forecasting. *J. Hydrometeor.*, 12, 713–728,
3 doi:10.1175/2011JHM1347.1.

4 Demeritt, D., Nobert, S., Cloke, H., and Pappenberger, F. 2010. Challenges in communicating
5 and 5 using ensembles in operational flood forecasting, *Meteorol. Appl.*, 17, 209–222.

6 De Roo A., Gouweleeuw B., Thielen J., Bartholmes J. et al. 2003. Development of a European
7 flood forecasting system. *International Journal of River Basin Management* 1(1): 49–59

8 DHI. MIKE 21 FM Flow model, Scientific documentation. 2014, DHI Group, Horslhome

9 Di Baldassarre G. 2012. Floods in a Changing Climate: Inundation Modelling. *International*
10 *Hydrology Series*, Cambridge University Press, Online ISBN:9781139088411, doi:
11 <http://dx.doi.org/10.1017/CBO9781139088411>

12 Di Baldassarre G., Schumann G., Bates P.D., Freer J.E., Beven K.J. 2010. Floodplain mapping:
13 a critical discussion of deterministic and probabilistic approaches, *Hydrological Sciences*
14 *Journal*, 55:3, 364-376, doi: 10.1080/02626661003683389.

15 Di Baldassarre, G., Montanari, A., Lins, H., et al. 2010b. Flood fatalities in Africa: from
16 diagnosis to mitigation. *Geophysical Research Letters*, 37, L22402,
17 doi:10.1029/2010GL045467

18 Domínguez M. R., Esquivel G. G., Méndez A. B., Mendoza R. A., Arganis J. M. L., Carrizosa
19 E. E., 2008. Manual del Modelo para pronóstico de escurrimiento. Instituto de Ingeniería.
20 Universidad Nacional Autónoma de México. ISBN 978-607-2-00316-3.

21 Ferraris L., Rudari R., Siccardi F. 2002. The uncertainty in the prediction of flash floods in the
22 Northern Mediterranean environment. *Journal of Hydrometeorology* 3: 714–727

23 Fowler HJ, Blenkinsop S, Tebaldi C. 2007a. Linking climate change modelling to impacts
24 studies: recent advances in downscaling techniques for hydrological modelling. *International*
25 *Journal of Climatology* 27: 1547–1578.

26 Giorgi, F. 1990. Simulation of regional climate using a limited area model nested in a general
27 circulation model, *J. Clim.*, 3, 941– 963.

28 Giorgi, F. 2006. Regional climate modeling: Status and perspectives, *J. Phys. IV*, 139, 101–
29 118.

1 Hacking, I. 2006 The emergence of probability, 2nd edn. New York, NY: Cambridge University
2 Press.

3 Horritt M.S., Bates P.D. 2002. Evaluation of one-dimensional and two-dimensional models for
4 predicting river flood inundation. *Journal of Hydrology* 268: 87–99.

5 Horritt M.S., Bates P.D., Mattinson M.J. 2006. Effects of mesh resolution and topographic
6 representation in 2D finite volume models of shallow water fluvial flow. *Journal of Hydrology*
7 329: 306–314. DOI:10.1016/j.jhydrol.2006.02.016.

8 Hunter, N. M., Bates, P. D., Horritt, M. S., et al. 2005. Utility of different data types for
9 calibrating flood inundation models within a GLUE framework. *Hydrology and Earth System*
10 *Sciences*, 9(4), 412–430.

11 Hunter, M., Bates, P.D., Neelz, S., Pender, G., Villanueva, I., Wright, N.G., Liang, D., Falconer,
12 A., Lin, B., Waller, S., Crossley, A.J., Mason, D.C., 2008, Benchmarking 2D hydraulic models
13 for urban flooding, *Water Management*, 161, Issue WM1, 13-30.

14 INEGI. 2008. Nube de Puntos LIDAR ajustada al Terreno, Bloque conformado por las cartas
15 1:50,000: E15A75, E15A76, E15A85, E15A86 del Instituto Nacional de Estadística, Geografía
16 e Informática, México.

17 Jankov, I., W. A. Gallus, et al. The Impact of Different WRF Model Physical Parameterizations
18 and Their Interactions on Warm Season MCS Rainfall. *Weather and Forecasting* 20, (2005):
19 1048-

20 Leung, L. R., and Y. Qian, 2009. Atmospheric rivers induced heavy precipitation and flooding
21 in the western U.S. simulated by the WRF regional climate model. *Geophysical Research*
22 *Letters*, 36, L03820, doi:10.1029/2008GL036445.

23 Liguori, S., Rico-Ramirez, M.A. 2012. Quantitative assessment of short-term rainfall forecasts
24 from radar nowcasts and MM5 forecasts. *Hydrological Processes*, vol 26., pp. 3842-3857

25 Liguori, S., Rico-Ramirez, M.A., Schellart, A., Saul, A. 2012, Using probabilistic radar rainfall
26 nowcasts and NWP forecasts for flow prediction in urban catchments. *Atmospheric Research*,
27 vol 103., pp. 80 – 95

28 Lo, J. C. F., Z. L. Yang, and R. A. Pielke Sr., 2008. Assessment of three dynamical climate
29 downscaling methods using the Weather Research and Forecasting (WRF) model. *Journal of*
30 *Geophysical Research*, 113, D09112, doi:10.1029/2007JD009216.

1 Milly P.C.D., Wetherland, R.T., Dunne, K.A., Delworth, T.L. 2002. Increasing risk of great
2 floods in a changing climate. *Nature*, Vol.415, 514-517, doi :10.1038/415514a

3 Pappenberger, F., Beven, K. J., Hunter, N. M., Bates P. D., Gouweleeuw, B. T., Thielen, J., de
4 Roo. A. P. J. 2005. Cascading model uncertainty from medium range weather forecasts (10
5 days) through a rainfall-runoff model to flood inundation predictions within the European Flood
6 Forecasting System (EFFS), *Hydrology and Earth System Sciences*, 9(4), pp. 381-393.
7 doi:10.5194/hess-9-381-2005

8 Pappenberger, F., Beven, K.J., Hunter N., Gouweleeuw, B., Bates, P., de Roo, A., Thielen, J.,
9 2005, Cascading model uncertainty from medium range weather forecasts (10 days) through a
10 rainfallrunoff model to flood inundation predictions within the European Flood Forecasting
11 System (EFFS). *Hydrology and Earth System Science*, 9(4), 381-393.

12 Pappenberger, F, Matgen, P, Beven, K J, Henry J-B, Pfister, L and de Fraipont, P, 2006,
13 Influence of uncertain boundary conditions and model structure on flood inundation
14 predictions, *Advances in Water Resources*, 29(10), 1430-
15 1449,doi:10.1016/j.advwatres.2005.11.012

16 Pappenberger, F., Beven, K.J., Frodsham, K., Romanovicz, R. and Matgen, P., 2007. Grasping
17 the unavoidable subjectivity in calibration of flood inundation models: a vulnerability weighted
18 approach. *Journal of Hydrology*, 333, 275-287.

19 Pappenberger, F., J. Bartholmes, J. Thielen, H. L. Cloke, R. Buizza, and A. de Roo (, 2008),
20 New dimensions in early flood warning across the globe using grand-ensemble weather
21 predictions, *Geophys. Res. Lett.*, 35, L10404, doi:10.1029/2008GL033837.

22 Pappenberger, F., Dutra, E., Wetterhall, F., Cloke, H. 2012. Deriving global flood hazard maps
23 of fluvial floods through a physical model cascade. *Hydrology and Earth System Sciences*, 16
24 4143–56.

25 Pedrozo-Acuña, A., Breña-Naranjo, J.A., Domínguez-Mora, R., 2014. The hydrological setting
26 of the 2013 floods in Mexico. *Weather*. Vol.69, No.11, 295-302 Wiley and Sons. doi:
27 10.1002/wea.2355

28 Pedrozo-Acuña A., Mariño-Tapia I., Enriquez Ortiz C., Medellín Mayoral G., González-
29 Villareal F.J. 2011. Evaluation of inundation areas resulting from the diversion of an extreme
30 discharge towards the sea: case study in Tabasco, Mexico. *Hydrological Processes*, 26, (5),
31 687–704.

- 1 Pedrozo-Acuña, A., Rodríguez-Rincón, J.P., Arganis-Juárez, M., Domínguez-Mora, R. and
2 González Villareal, F.J. 2013. Estimation of probabilistic flood inundation maps for an extreme
3 event: Pánuco River, México. *Journal of Flood Risk Management*, doi: 10.1111/jfr3.12067
- 4 Pedrozo-Acuña, A., Ruiz de Alegria-Arzaburu, A., Mariño-Tapia, I., Enriquez, C., González-
5 Villareal, F.J. 2012. Factors controlling flooding at the Tonalá river mouth (Mexico). *Journal*
6 *of Flood Risk Management*, Vol.5 (3) pp 226-244. doi: 10.1111/j.1753-318X.2012.01142.x
- 7 Pedrozo-Acuña, A. Mejía-Estrada P.I., Rodríguez-Rincón, J.P., Domínguez-Mora, R.,
8 González-Villareal, F.J., *Flood Risk From Extreme Events in Mexico*, 11th International
9 Conference on Hydroinformatics, 2014b.
- 10 Prinos P., Kortenhaus A., Swerpel B. & Jiménez J.A. 2008. Review of flood hazard mapping.
11 Floodsite Report No. T03-07-01, 54.
- 12 Qian, J.-H., A. Seth, and S. Zebiak 2003. Reinitialized versus continuous simulations for
13 regional climate downscaling, *Mon. Weather Rev.*, 131, 2857–2874.
- 14 Rodríguez-Rincón, J.P., Pedrozo-Acuña, A., Domínguez Mora, R., Reeve, D.E., Cluckie, I.
15 2012. Probabilistic estimation of flood maps: An ensemble approach. *FloodRisk2012*, The 2nd
16 European Conference on FLOODrisk Management.
- 17 [Romanowicz, R. and Beven, K. J., 2003, Bayesian estimation of flood inundation probabilities](#)
18 [as conditioned on event inundation maps, *Water Resources Research*, 39\(3\), W01073,](#)
19 [10.1029/2001WR001056.](#)
- 20 Skamarock, W.C., Klemp, J.B., Dudhia, J., Gill, D.O., Barker, D.M., Duda, M.G., Huang, X.-
21 Y., Wang, W., Powers, J.G. 2008. *A description of the Advanced Research WRF version3*.
22 NCAR Technical Note NCAR/TN475+STR.
- 23 Slingo, J., Belcher, S., Scaife, A., McCarthy, M., Saulter, A., McBeath, K., Jenkins, A.,
24 Huntingford, C., Marsh, T., Hannaford, J., Parry, S. 2014. The recent storms and floods in the
25 UK. Report Met Office and CEH.
- 26 Teutschbein C, Seibert J. 2010. Regional climate models for hydrological impact studies at the
27 catchment scale: a review of recent modelling strategies. *Geography Compass* 4: 834–860.
- 28 USDA-SCS. 1985. *National Engineering Handbook, Section 4 - Hydrology*. Washington, D.C.:
29 USDA-SCS.

1 Ushiyama, T., Sayama, T., Tatebe, Y., Fujioka, S., Fukami, K., 2014. Numerical simulation of
2 2010 Pakistan Flood in the Kabul river basin by using lagged ensemble rainfall forecasting,
3 Journal of Hydrometeorology, Vol. 15, 193-211 pp., doi: 10.1175/JHM-D-13-011.1.

4 Ven den Honert, R. C. & McAneney, J. 2011. The 2011 Brisbane floods: Causes, impacts and
5 implications. Water 3, 1149–1173.

6 Wang, W., Bruyere, C., Duda, M., Dudhia, J., Gill, D., Lin, H. C., & Mandel, J.. *ARW version*
7 *3 modeling system user's guide*. Mesoscale & Microscale Meteorology Division. National
8 Center for Atmospheric Research (July 2010), http://www.mmm.ucar.edu/wrf/users/docs/user_guide_V3/ARWUsersGuideV3.pdf.

10 Ward, P. J., De Moel, H., and Aerts, J. C. J. H. 2011 How are flood risk estimates affected by
11 the choice of return-periods? Nat. Hazards Earth Syst. Sci. 11 3181–95.

12 Webster, P. J., Toma, V. E. & Kim, H. M. 2011. Were the 2010 Pakistan floods predictable?
13 Geophys. Res. Lett. 38, L04806.

14 Werner, M.G.F., Hunter, N. and Bates, P.D. 2005. Identifiability of distributed floodplain
15 roughness values in flood extent estimation, J. Hydrol., 314, 139–157.

16 World Meteorological Organization, 2011. Provisional Statement on the Status of the Global
17 Climate; available http://www.wmo.int/pages/mediacentre/press_releases/gcs_2011_en.html

18 Wright, N. G., Asce, M., Villanueva, I., et al. (2008). Case study of the use of remotely sensed
19 data for modeling flood inundation on the River Severn, UK. Journal of Hydraulic Engineering,
20 134(5), 533–540.

21 Ye, J., He, Y., Pappenberger, F., Cloke, H. L., Manful, D. Y. and Li, Z. (2014), Evaluation of
22 ECMWF medium-range ensemble forecasts of precipitation for river basins. Q.J.R. Meteorol.
23 Soc., 140: 1615–1628. doi: 10.1002/qj.2243

24

1

2

Table 1. Ensemble members defined for the multi-physics WRF ensemble

Ensemble member	Micro-Physics	surface layer physics	Cumulus physics	Feedback /sst_update	RMSE	NSC	Cor	Bias	Criteria NSC >0.3, Cor >0.8
1	WSM5	5-Layer TDM	Kain-Fritsch Eta	off/off	445.23	-0.25	0.94	0.44	reject
2	WSM5	5-Layer TDM	Kain-Fritsch Eta	off/on	262.73	0.44	0.97	0.98	select
3	WSM5	5-Layer TDM	Kain-Fritsch Eta	on/off	250.51	0.49	0.97	1.01	select
4	WSM5	5-Layer TDM	Kain-Fritsch Eta	on/on	257.35	0.43	0.97	1.05	select
5	WSM5	5-Layer TDM	Betts-Miller-Janjic	off/on	502.47	-0.65	0.97	0.28	reject
6	WSM5	5-Layer TDM	Betts-Miller-Janjic	on/on	520.58	-0.77	0.97	0.25	reject
7	WSM5	Noah	Kain-Fritsch Eta	off/off	233.04	0.42	0.96	1.18	select
8	WSM5	Noah	Kain-Fritsch Eta	off/on	236.14	0.33	0.96	1.24	select
9	WSM5	Noah	Kain-Fritsch Eta	on/off	359.11	0.17	0.90	0.56	reject
10	WSM5	Noah	Kain-Fritsch Eta	on/on	245.31	0.41	0.96	1.12	select
11	WSM5	Noah	Betts-Miller-Janjic	off/off	486.26	-0.49	0.98	0.33	reject
12	WSM5	Noah	Betts-Miller-Janjic	off/on	486.02	-0.49	0.97	0.34	reject
13	WSM5	Noah	Betts-Miller-Janjic	on/off	535.00	-0.82	0.97	0.23	reject
14	WSM5	Noah	Betts-Miller-Janjic	on/on	543.78	-0.87	0.96	0.23	reject
15	Thompson	5-Layer TDM	Kain-Fritsch Eta	off/off	216.70	0.60	0.97	1.09	select
16	Thompson	5-Layer TDM	Kain-Fritsch Eta	off/on	236.64	0.50	0.97	1.15	select
17	Thompson	5-Layer TDM	Kain-Fritsch Eta	on/off	238.89	0.57	0.96	0.97	select
18	Thompson	5-Layer TDM	Kain-Fritsch Eta	on/on	275.24	0.50	0.96	0.89	select
19	Thompson	5-Layer TDM	Betts-Miller-Janjic	off/on	571.49	-1.15	0.96	0.16	reject
20	Thompson	5-Layer TDM	Betts-Miller-Janjic	on/off	572.27	-1.14	0.95	0.16	reject
21	Thompson	5-Layer TDM	Betts-Miller-Janjic	on/on	502.47	-0.65	0.97	0.28	reject
22	Thompson	Noah	Kain-Fritsch Eta	off/off	238.06	0.38	0.96	1.25	select
23	Thompson	Noah	Kain-Fritsch Eta	off/on	234.03	0.48	0.97	1.13	select

3

4

5

6

1 Table 2. Error Metrics in the estimation of precipitation by members of the multi-physics ensemble (blue rows
 2 indicate the stations located within the Tonalá catchment)

Root-Mean Square Error (RMSE) and Normalised RMSE per Station considering Ensemble average													
Station No.	Multi-physics ensemble member												<Nor_RMSE> %
	M1	M2	M3	M4	M5	M6	M7	M8	M9	M10	M11	M12	
30167	210.26	96.56	144.62	104.42	106.84	76.31	160.48	129.88	101.03	210.95	164.85	86.80	13.96
27003	544.34	578.19	564.46	474.81	427.30	516.95	458.25	484.05	568.20	572.30	385.17	479.47	35.13
27007	234.90	246.00	198.01	135.27	129.43	207.93	126.51	197.32	246.90	328.28	132.09	191.81	19.44
27015	96.68	129.89	151.02	194.33	235.76	179.69	152.06	152.60	118.97	116.87	260.49	188.20	24.01
27074	173.37	211.87	191.22	197.46	78.94	148.88	174.92	247.65	187.98	207.39	123.09	157.21	17.19
27073	227.47	201.91	228.62	256.39	281.38	245.68	186.21	219.36	159.34	147.79	247.69	223.88	46.46
27075	87.04	119.26	104.10	100.82	151.17	64.92	76.45	147.30	85.75	105.68	52.14	68.67	10.72
27076	140.53	160.28	141.95	124.03	108.33	130.53	191.75	162.59	226.04	236.09	129.78	150.84	17.14
27077	89.10	113.42	83.60	225.48	252.24	207.73	254.20	282.40	110.77	83.93	203.01	192.86	30.57
27039	333.50	204.36	197.48	295.84	302.19	261.39	264.08	321.66	172.86	152.14	257.59	430.63	73.28
27054	123.18	30.77	45.28	113.16	119.18	77.41	106.84	112.68	118.83	127.43	110.06	106.67	34.75
27060	70.69	56.23	59.51	33.42	40.13	30.04	78.07	93.80	88.46	80.36	56.73	66.31	19.88
27024	160.33	137.81	140.76	120.58	127.54	73.57	148.27	136.47	145.12	167.79	153.26	151.87	85.04
27084	68.72	71.32	54.58	53.56	106.93	65.65	61.06	72.31	61.46	62.96	50.14	50.92	19.02
7365	172.91	117.44	103.02	252.03	139.79	163.49	301.52	216.38	179.67	129.71	271.88	210.11	24.52
27011	143.70	162.77	143.61	107.82	77.55	86.15	128.03	143.69	106.59	116.49	86.81	81.27	106.83
27036	81.46	60.69	27.36	61.69	19.14	35.64	23.58	45.89	22.13	40.23	39.22	55.55	12.04
27008	158.85	72.82	74.96	131.34	134.94	100.16	102.82	149.97	66.67	79.36	97.87	254.33	19.68
Average {Rel_RMSE} catch.												23.14	
Average {Rel_RMSE} all												33.87	

BIAS per Station and Ensemble Average													
Station No.	Multi-physics ensemble member												<BIAS>
	M1	M2	M3	M4	M5	M6	M7	M8	M9	M10	M11	M12	
30167	0.71	0.90	0.81	1.07	1.12	0.99	0.80	0.85	0.91	0.71	1.23	1.06	0.93
27003	0.51	0.48	0.50	0.58	0.62	0.54	0.59	0.57	0.49	0.49	0.66	0.58	0.55
27007	0.72	0.71	0.79	0.91	0.91	0.78	1.13	1.26	0.73	0.61	0.90	0.80	0.85
27015	1.21	1.32	1.40	1.50	1.61	1.46	1.37	1.37	1.24	1.21	1.68	1.48	1.40
27074	0.82	0.76	0.79	0.78	1.08	0.86	0.81	0.71	0.80	0.77	0.88	0.83	0.82
27073	1.74	1.65	1.74	1.83	1.91	1.80	1.58	1.70	1.47	1.44	1.80	1.72	1.70
27075	0.92	0.85	0.88	0.88	1.20	0.96	0.90	0.80	0.89	0.86	0.98	0.93	0.92
27076	0.86	0.82	0.86	0.91	0.95	0.89	0.79	0.84	0.73	0.71	0.89	0.85	0.84
27077	1.12	1.17	1.10	1.48	1.54	1.44	1.54	1.60	1.20	1.14	1.42	1.40	1.35
27039	2.41	1.87	1.84	2.26	2.29	2.11	2.13	2.36	1.73	1.64	2.09	2.84	2.13
27054	1.89	1.08	1.24	1.82	1.87	1.54	1.76	1.81	1.84	1.91	1.79	1.77	1.69
27060	1.42	1.33	0.72	1.08	1.20	1.05	1.47	1.57	1.54	1.49	1.32	1.39	1.30
27024	3.34	2.96	3.03	2.76	2.88	2.07	3.16	2.98	3.11	3.45	3.17	3.17	3.01
27084	1.32	1.35	1.17	1.23	1.61	0.78	1.27	1.36	1.27	1.29	1.07	1.01	1.23
7365	1.43	1.20	1.09	1.63	1.32	0.72	1.78	1.55	1.43	1.26	1.68	1.51	1.38
27011	3.57	3.91	3.55	2.93	2.33	2.49	3.33	3.58	2.91	3.09	2.56	2.45	3.06
27036	1.36	1.25	1.09	1.28	0.97	1.15	0.95	1.20	1.06	1.16	1.15	1.24	1.15
27008	1.37	1.07	1.05	1.29	1.31	1.20	1.21	1.35	0.99	0.93	1.19	1.62	1.22
Average {Rel_RMSE} catch.												0.94	
Average {Rel_RMSE} all												1.42	

3
 4
 5
 6

1 Continuation of Table 2. Error Metrics in the estimation of precipitation by members of the multi-physics
 2 ensemble (blue rows indicate the stations located within the Tonalá catchment)
 3

Nash-Sutcliff Coefficient per Station and Ensemble average													
Station No.	Multi-physics ensemble member												<NSC>
	M1	M2	M3	M4	M5	M6	M7	M8	M9	M10	M11	M12	
30167	0.72	0.94	0.87	0.93	0.93	0.96	0.84	0.89	0.94	0.72	0.83	0.95	0.88
27003	0.16	0.05	0.09	0.36	0.48	0.24	0.40	0.33	0.08	0.07	0.58	0.34	0.26
27007	0.70	0.67	0.78	0.90	0.91	0.76	0.91	0.79	0.66	0.41	0.90	0.80	0.77
27015	0.88	0.78	0.70	0.50	0.27	0.57	0.70	0.69	0.81	0.82	0.11	0.53	0.61
27074	0.84	0.76	0.80	0.79	0.97	0.88	0.84	0.67	0.81	0.77	0.92	0.87	0.83
27073	-0.27	0.00	-0.28	-0.61	-0.94	-0.48	0.15	-0.18	0.38	0.46	-0.50	-0.23	-0.21
27075	0.94	0.89	0.91	0.92	0.82	0.97	0.95	0.83	0.94	0.91	0.98	0.96	0.92
27076	0.87	0.83	0.86	0.90	0.92	0.88	0.75	0.82	0.65	0.62	0.89	0.85	0.82
27077	0.82	0.70	0.84	-0.17	-0.46	0.01	-0.48	-0.83	0.72	0.84	0.05	0.15	0.18
27039	-4.41	-1.03	-0.90	-3.26	-3.44	-2.32	-2.39	-4.03	-0.45	-0.13	-2.23	-8.02	-2.72
27054	-0.46	0.91	0.80	-0.23	-0.36	0.42	-0.10	-0.22	-0.36	-0.56	-0.16	-0.09	-0.03
27060	0.60	0.75	0.72	0.91	0.87	0.93	0.51	0.29	0.37	0.48	0.74	0.65	0.65
27024	-7.99	-5.64	-5.93	-4.08	-4.69	-0.89	-6.68	-5.51	-6.36	-8.84	-7.21	-7.06	-5.91
27084	0.67	0.64	0.79	0.80	0.20	0.70	0.74	0.63	0.73	0.72	0.82	0.82	0.69
7365	0.50	0.77	0.82	-0.07	0.67	0.55	-0.54	0.21	0.45	0.72	-0.25	0.25	0.34
27011	-16.74	-21.76	-16.72	-8.99	-4.17	-5.38	-13.08	-16.74	-8.76	-10.66	-5.47	-4.67	-11.09
27036	0.61	0.78	0.96	0.78	0.98	0.93	0.97	0.88	0.97	0.91	0.91	0.82	0.87
27008	0.60	0.92	0.91	0.72	0.71	0.84	0.83	0.64	0.93	0.90	0.85	-0.03	0.73
Average {Rel_RMSE} catch.												0.63	
Average {Rel_RMSE} all												-0.63	

Correlation Coefficient per Station and Ensemble average													
Station No.	Multi-physics ensemble member												<Cor>
	M1	M2	M3	M4	M5	M6	M7	M8	M9	M10	M11	M12	
30167	0.99	0.99	0.99	0.97	0.98	0.99	0.99	0.99	0.99	0.99	0.97	0.98	0.99
27003	0.95	0.96	0.97	0.97	0.98	0.98	0.99	0.99	0.99	0.99	0.99	0.99	0.98
27007	0.98	0.97	0.97	0.97	0.97	0.97	0.97	0.97	0.97	0.95	0.98	0.97	0.97
27015	0.97	0.96	0.97	0.94	0.93	0.95	0.95	0.95	0.94	0.94	0.93	0.94	0.95
27074	0.98	0.98	0.98	0.98	0.99	0.98	0.99	0.98	0.98	0.98	0.99	0.99	0.98
27073	0.95	0.96	0.95	0.94	0.94	0.94	0.92	0.92	0.91	0.92	0.94	0.94	0.94
27075	0.98	0.98	0.98	0.98	0.99	0.99	0.99	0.99	0.99	0.99	0.99	0.99	0.99
27076	0.98	0.98	0.97	0.97	0.97	0.97	0.97	0.97	0.96	0.96	0.97	0.97	0.97
27077	0.96	0.95	0.96	0.96	0.95	0.96	0.95	0.95	0.97	0.97	0.95	0.96	0.96
27039	0.95	0.95	0.94	0.93	0.94	0.94	0.94	0.94	0.95	0.95	0.94	0.93	0.94
27054	0.91	0.96	0.94	0.93	0.93	0.94	0.91	0.92	0.91	0.90	0.93	0.93	0.93
27060	0.96	0.97	0.97	0.96	0.97	0.97	0.95	0.95	0.96	0.96	0.97	0.96	0.96
27024	0.91	0.93	0.92	0.90	0.91	0.95	0.89	0.90	0.89	0.89	0.94	0.94	0.91
27084	0.91	0.91	0.92	0.94	0.92	0.95	0.92	0.91	0.92	0.92	0.93	0.93	0.92
7365	0.93	0.93	0.94	0.92	0.94	0.97	0.91	0.92	0.91	0.92	0.91	0.92	0.93
27011	0.94	0.94	0.95	0.93	0.95	0.96	0.89	0.93	0.91	0.92	0.91	0.91	0.93
27036	0.99	0.99	0.99	0.99	0.99	0.99	0.99	0.99	0.99	0.99	0.99	0.99	0.99
27008	0.97	0.96	0.96	0.96	0.96	0.96	0.96	0.96	0.97	0.96	0.96	0.96	0.96
Average {Rel_RMSE} catch.												0.97	
Average {Rel_RMSE} all												0.95	

4

1
2
3
4
5
6
7

Table 3. Flood events in the Tonalá River used in the calibration process of free parameters in the hydrological model, along with computed error metrics.

Event	Max Q (m ³ /s) Obs.	λ	Fs	Fo	Max Q (m ³ /s) Calc.	NSC	Cor	Bias
2001	577.98	0.2	0.1	0.9	584.79	0.529	0.764	1.112
2005	589.25	0.4	0.6	0.9	609.87	0.812	0.907	1.043
2007	538.50	0.2	1.8	0.9	543.87	0.483	0.780	0.902
2008	597.35	0.4	1.8	0.9	823.04	0.155	0.861	0.983
2009	1262.57	0.8	1.8	0.9	1424.56	0.910	0.962	0.942
2011	545.40	0.9	1.6	0.9	597.08	0.413	0.721	1.051

8

1 Table 4. Error metrics in the estimation of river discharge by the rainfall-runoff model using 6 parameter sets and
 2 12 members of the multi-physics ensemble (those selected are shown in bold with NSC>0.6 and Cor>0.7).

Member No.	WRF Member	Hydrological Parameters	NSC	Cor	Bias
1	M1	2001	0.733	0.884	0.852
2	M2	2001	0.074	0.973	1.529
3	M3	2001	-0.035	0.974	1.564
4	M4	2001	-0.511	0.975	1.686
5	M5	2001	-0.638	0.441	1.485
6	M6	2001	-0.223	0.961	1.593
7	M7	2001	-0.192	0.961	1.579
8	M8	2001	-0.043	0.959	1.537
9	M9	2001	0.064	0.958	1.504
10	M10	2001	0.245	0.971	0.525
11	M11	2001	-1.503	0.944	1.832
12	M12	2001	-0.752	0.954	1.710
13	M1	2005	0.639	0.901	0.742
14	M2	2005	0.404	0.977	1.414
15	M3	2005	0.318	0.978	1.449
16	M4	2005	-0.077	0.977	1.569
17	M5	2005	-0.545	0.366	1.368
18	M6	2005	0.181	0.968	1.478
19	M7	2005	0.200	0.968	1.465
20	M8	2005	0.321	0.966	1.422
21	M9	2005	0.408	0.966	1.389
22	M10	2005	-0.081	0.960	0.426
23	M11	2005	-0.909	0.951	1.717
24	M12	2005	-0.264	0.961	1.595
25	M1	2007	0.376	0.914	0.601
26	M2	2007	0.761	0.978	1.244
27	M3	2007	0.711	0.979	1.278
28	M4	2007	0.444	0.976	1.395
29	M5	2007	-0.440	0.261	1.191
30	M6	2007	0.633	0.974	1.306
31	M7	2007	0.647	0.974	1.293
32	M8	2007	0.722	0.973	1.251
33	M9	2007	0.771	0.972	1.219
34	M10	2007	-0.508	0.952	0.322
35	M11	2007	-0.129	0.959	1.539
36	M12	2007	0.340	0.969	1.420
37	M1	2008	0.240	0.922	0.547
38	M2	2008	0.837	0.978	1.186
39	M3	2008	0.797	0.978	1.220
40	M4	2008	0.570	0.974	1.337
41	M5	2008	-0.479	0.209	1.132
42	M6	2008	0.741	0.976	1.248
43	M7	2008	0.753	0.976	1.235
44	M8	2008	0.813	0.975	1.194
45	M9	2008	0.851	0.975	1.161
46	M10	2008	-0.720	0.945	0.276
47	M11	2008	0.079	0.962	1.481
48	M12	2008	0.495	0.972	1.361
49	M1	2009	-0.036	0.838	0.494
50	M2	2009	0.819	0.978	0.882
51	M3	2009	0.899	0.977	0.907
52	M4	2009	0.649	0.963	1.286
53	M5	2009	0.060	0.811	0.580
54	M6	2009	0.839	0.959	0.849
55	M7	2009	0.883	0.959	0.890
56	M8	2009	0.896	0.954	0.929
57	M9	2009	0.890	0.950	0.928
58	M10	2009	-1.233	0.972	0.209
59	M11	2009	0.638	0.938	1.236
60	M12	2009	0.885	0.946	1.042
61	M1	2011	-0.247	0.949	0.396
62	M2	2011	0.938	0.970	1.019
63	M3	2011	0.930	0.971	1.052
64	M4	2011	0.819	0.964	1.168
65	M5	2011	-0.662	0.055	0.955
66	M6	2011	0.890	0.978	1.133
67	M7	2011	0.899	0.979	1.120
68	M8	2011	0.931	0.979	1.079
69	M9	2011	0.945	0.978	1.047
70	M10	2011	-1.136	0.931	0.195
71	M11	2011	0.433	0.967	1.364
72	M12	2011	0.738	0.976	1.246
<Ensemble average of selected members>			0.793	0.965	1.113

3

1

2

3

Table 5. Error metrics in the estimation of river discharge by the hydrodynamic model using the 31 members of the multi-physics ensemble.

Comparison of flooded areas between numerical results from running ensemble members vs. Observed																																
Error metrics	Ensemble Member																												<Ensemble average>			
	M1	M13	M26	M27	M30	M31	M32	M33	M38	M39	M42	M43	M44	M45	M50	M51	M52	M54	M55	M56	M57	M59	M60	M62	M63	M64	M66	M67		M68	M69	M72
BIAS	0.903	0.838	1.084	1.099	1.119	1.120	1.094	1.078	1.056	1.021	1.092	1.089	1.096	1.051	0.902	0.915	0.891	0.820	1.020	0.982	0.872	1.056	1.004	0.982	0.995	1.047	1.040	1.028	1.016	1.005	1.092	1.013
FAR: False Alarm Ratio	0.148	0.120	0.215	0.217	0.283	0.210	0.216	0.212	0.209	0.217	0.216	0.215	0.152	0.207	0.148	0.154	0.139	0.137	0.193	0.155	0.133	0.206	0.187	0.178	0.182	0.204	0.201	0.225	0.192	0.187	0.216	0.189
POD: Probability of Detection	0.770	0.737	0.851	0.861	0.849	0.849	0.858	0.849	0.836	0.751	0.857	0.854	0.848	0.833	0.769	0.775	0.751	0.810	0.823	0.845	0.756	0.847	0.816	0.807	0.814	0.833	0.831	0.821	0.821	0.818	0.857	0.819
POFD: Probability of False Detection	0.124	0.094	0.217	0.222	0.187	0.187	0.220	0.214	0.205	0.186	0.220	0.219	0.186	0.203	0.124	0.131	0.185	0.185	0.184	0.066	0.108	0.266	0.175	0.163	0.168	0.199	0.195	0.186	0.182	0.175	0.220	0.180
CSI : Critical Success Index	0.679	0.670	0.690	0.695	0.711	0.711	0.694	0.691	0.685	0.709	0.693	0.692	0.710	0.685	0.679	0.679	0.706	0.654	0.687	0.708	0.677	0.620	0.687	0.687	0.690	0.686	0.687	0.619	0.688	0.688	0.693	0.686
True Skill Statistics	0.645	0.643	0.634	0.639	0.621	0.662	0.638	0.636	0.631	0.660	0.637	0.636	0.661	0.631	0.645	0.643	0.615	0.601	0.639	0.659	0.648	0.660	0.641	0.644	0.640	0.634	0.636	0.610	0.640	0.642	0.637	0.639

4

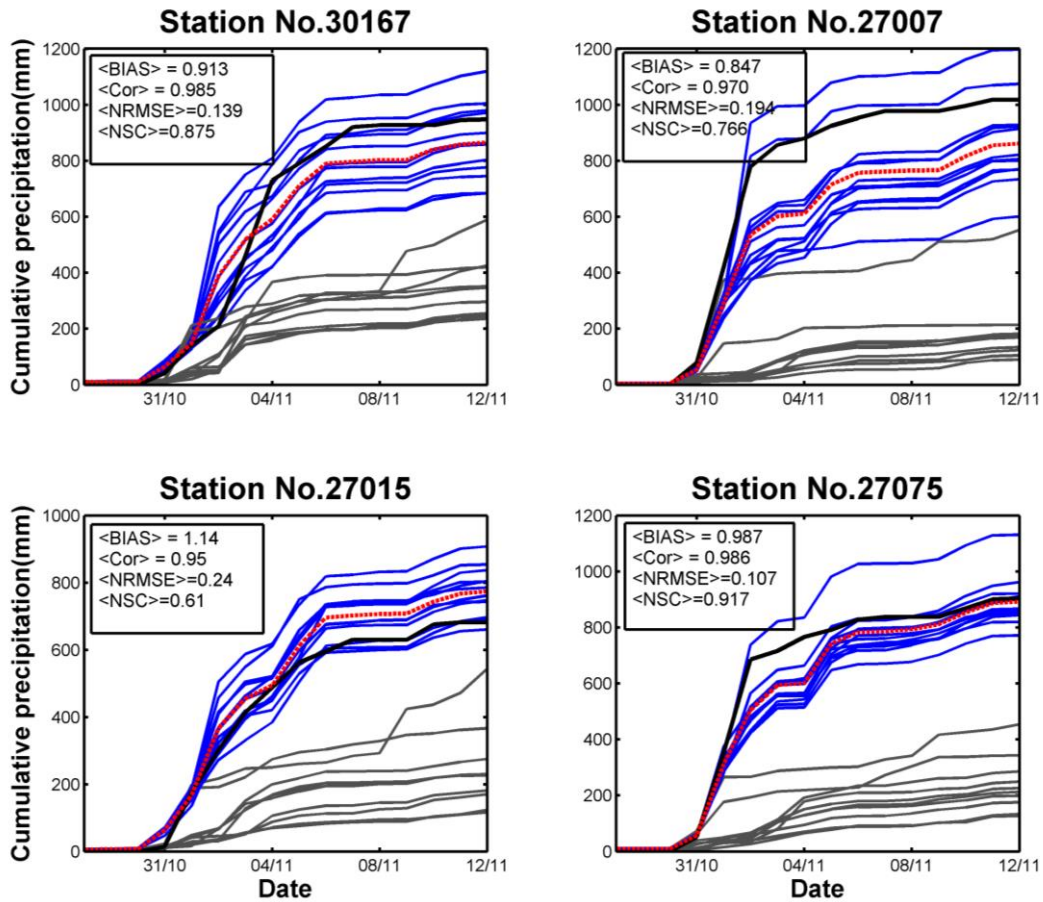
5

1
2
3
4
5
6
7
8
9
10
11
12
13
14
15
16
17



Figure 2. Numerical setup of the WRF with a nested domain covering Mexico. Domain 1: 25km resolution; Domain 2: 4km resolution; the orange region illustrates the Tonalá catchment.

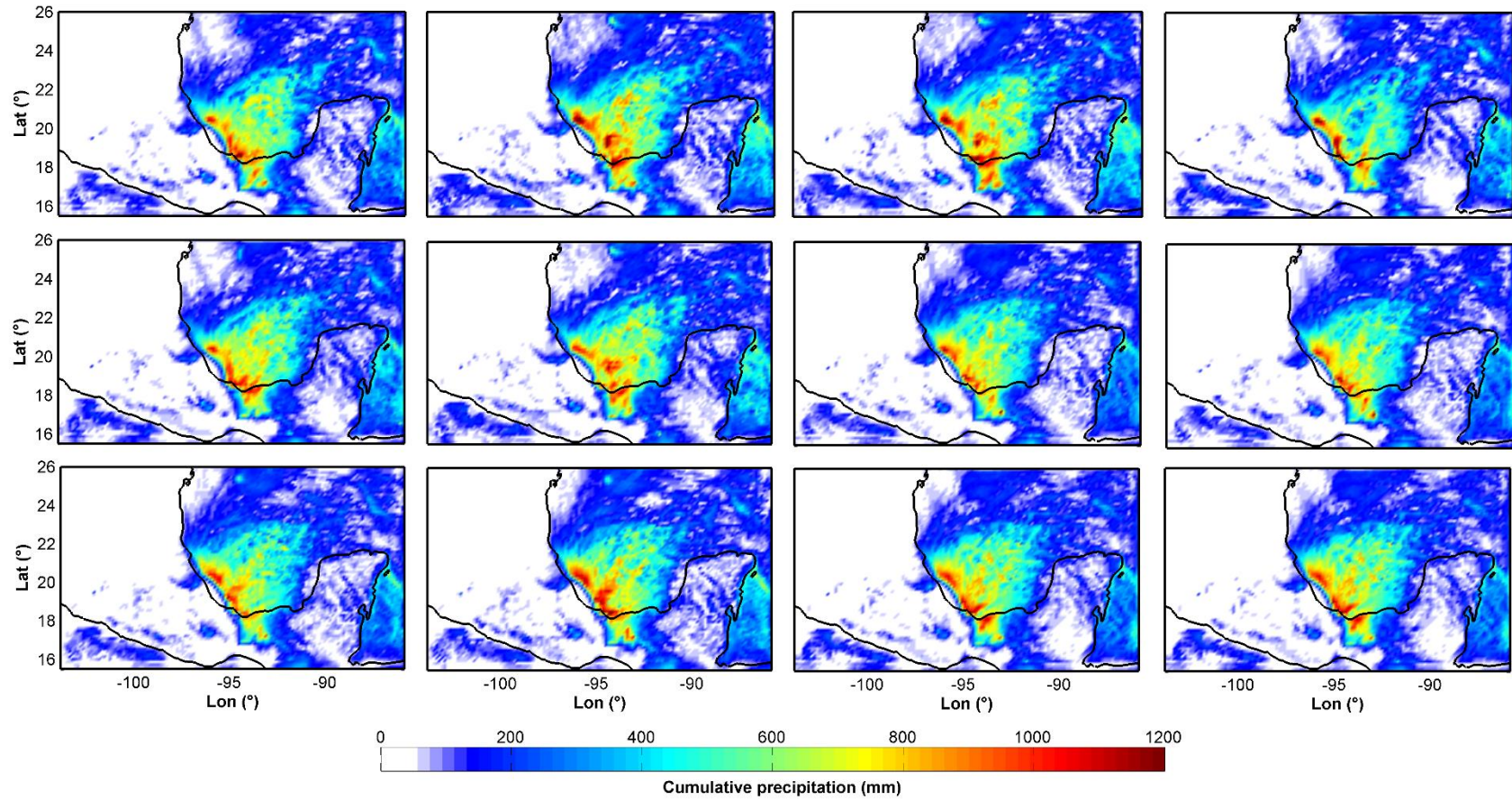
1
2



3
4
5
6
7
8

Figure 3. Comparison of cumulative precipitation estimated by the 23 model runs of the WRF multi-physics ensemble. Blue solid line: selected members with NSC > 0.3; grey solid line: disregarded members with NSC < 0.3; red dotted line: mean of the selected 12 members; black solid line: measurements at each of the four weather stations from 27th October 2009 to 12th November 2009.

1



2

3

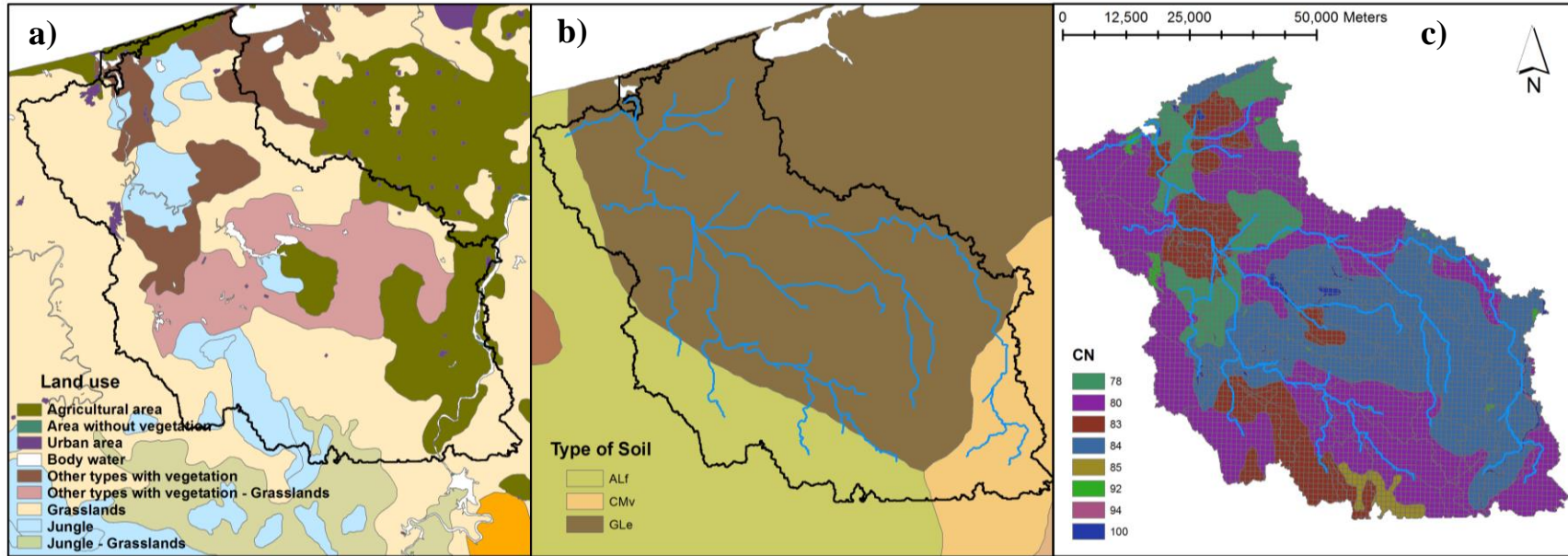
4

5

Figure 4. Cumulative precipitation fields estimated by the WRF model using the selected 12 members of the multi-physics ensemble (27th October 2009 – 12th November 2009).

1

2

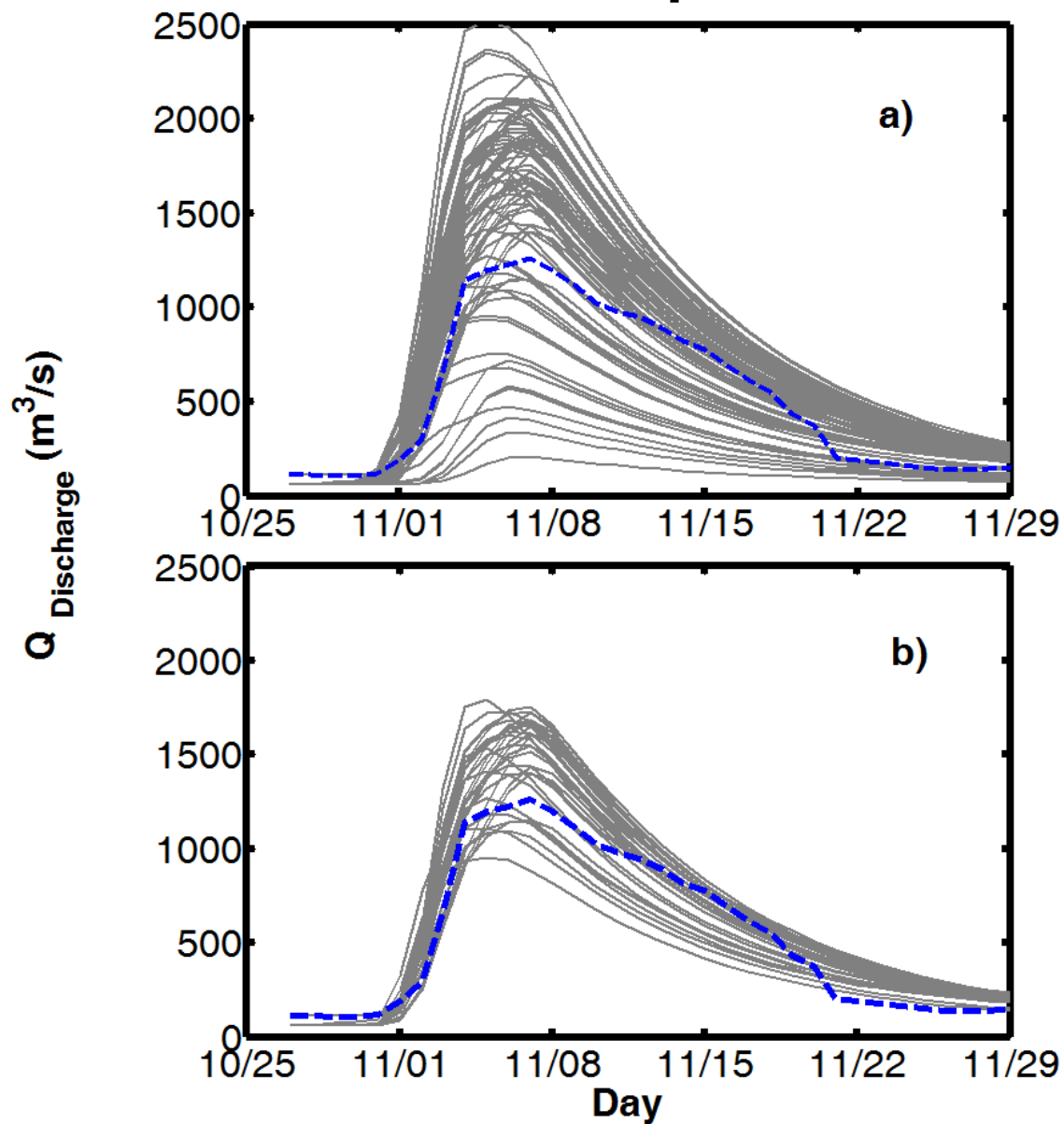


3

4

Figure 5. Input data parameters in the hydrological model; a) Land use; b) Pedology; c) River network, curve number and grid.

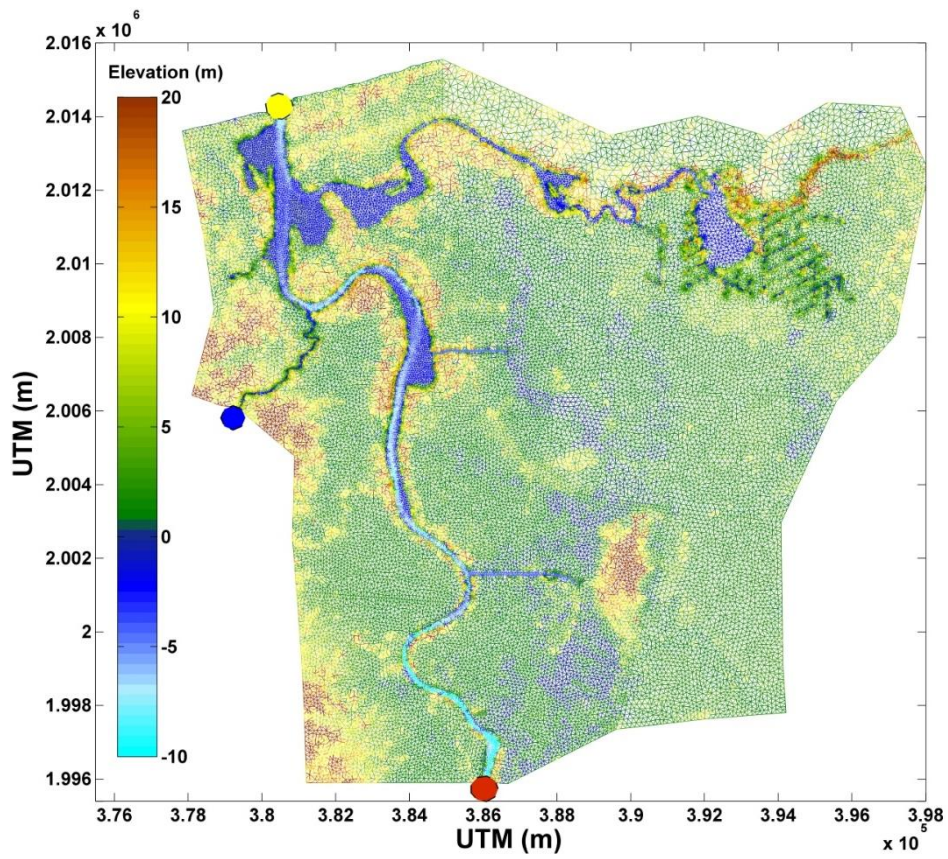
1
2



3
4
5
6
7
8

Figure 6. a) 72 hydrographs computed using the rainfall-runoff model with 6 sets of parameters and 12 WRF ensemble precipitation fields as input data; b) 31 selected hydrographs to serve as input in the hydrodynamic model; grey lines illustrate the ensemble members and the blue dashed line shows the measured river discharge for the event.

1



2

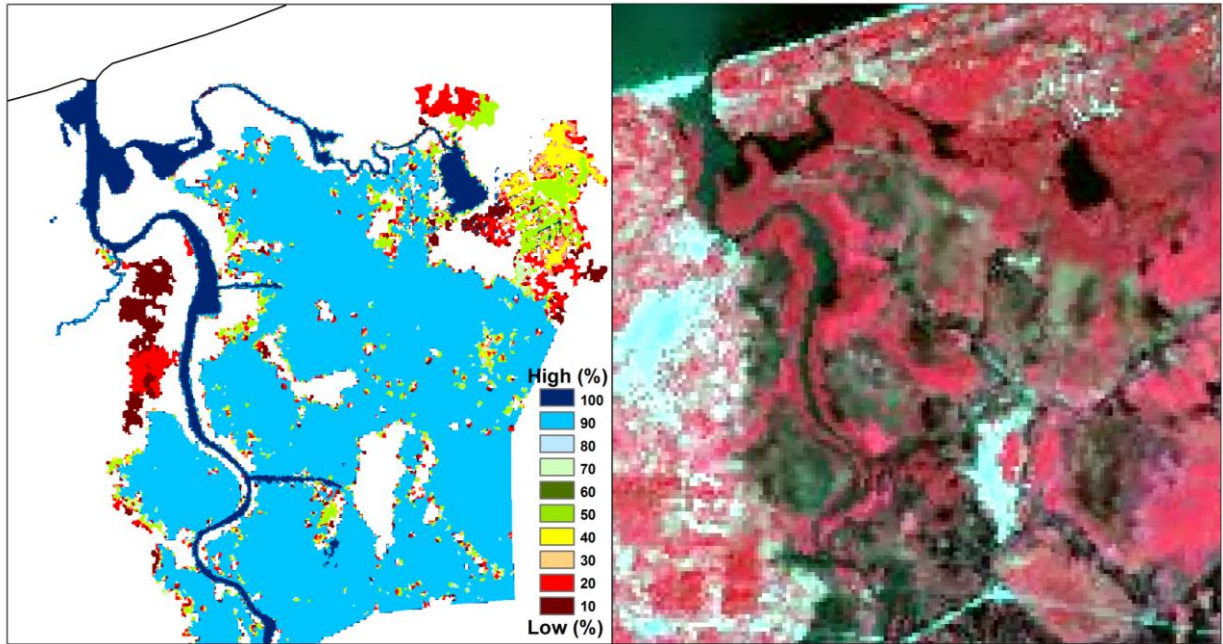
3

Figure 7. Model domain along with the numerical mesh and elevation data in the study area; Boundary conditions are represented by blue dot: Agua Dulcita river; red dot: input hydrograph; yellow dot: river-mouth.

5

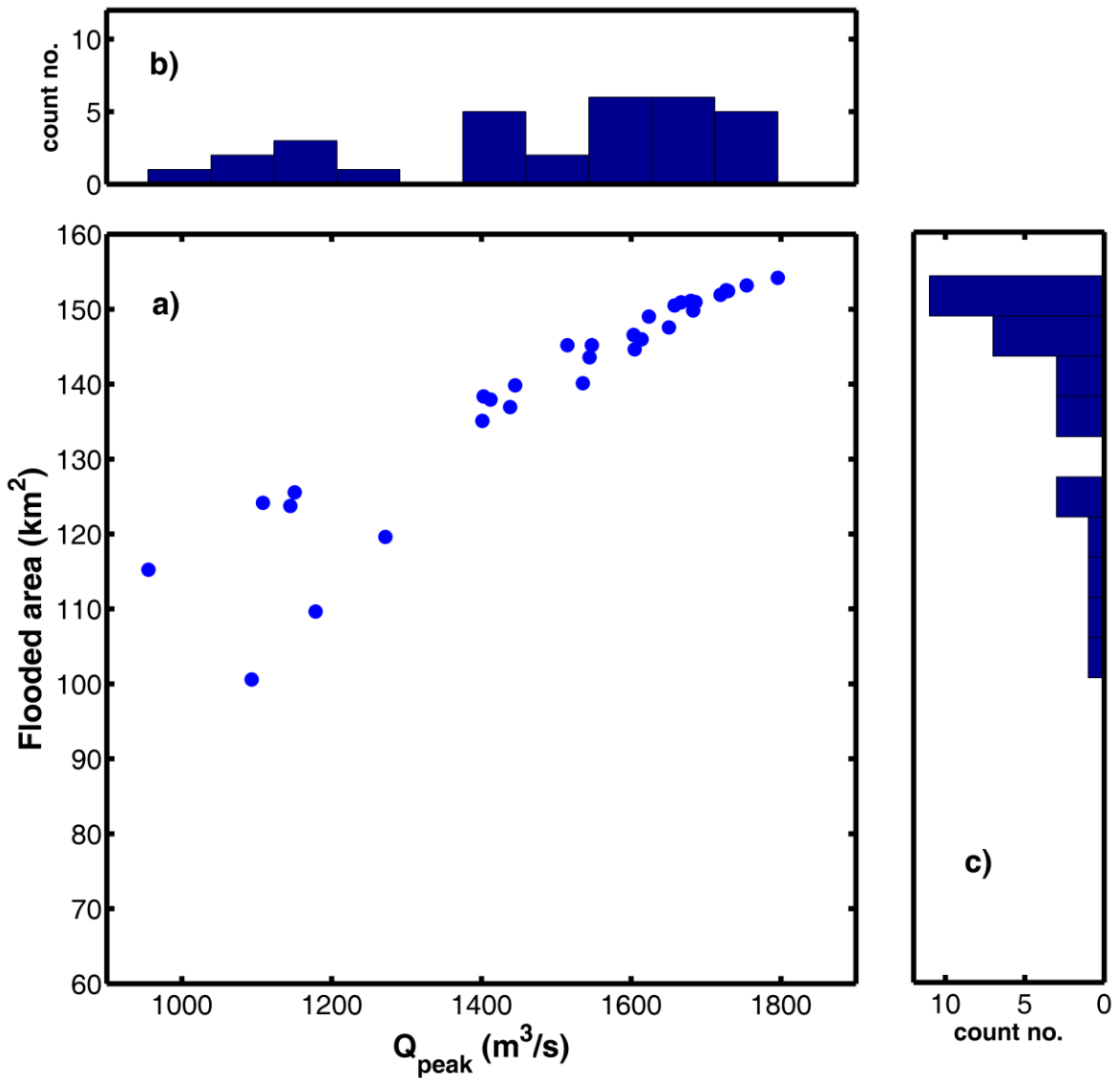
6

1
2
3
4
5



6
7
8
9
10
11
12
13
14
15
16
17
18
19
20
21
22

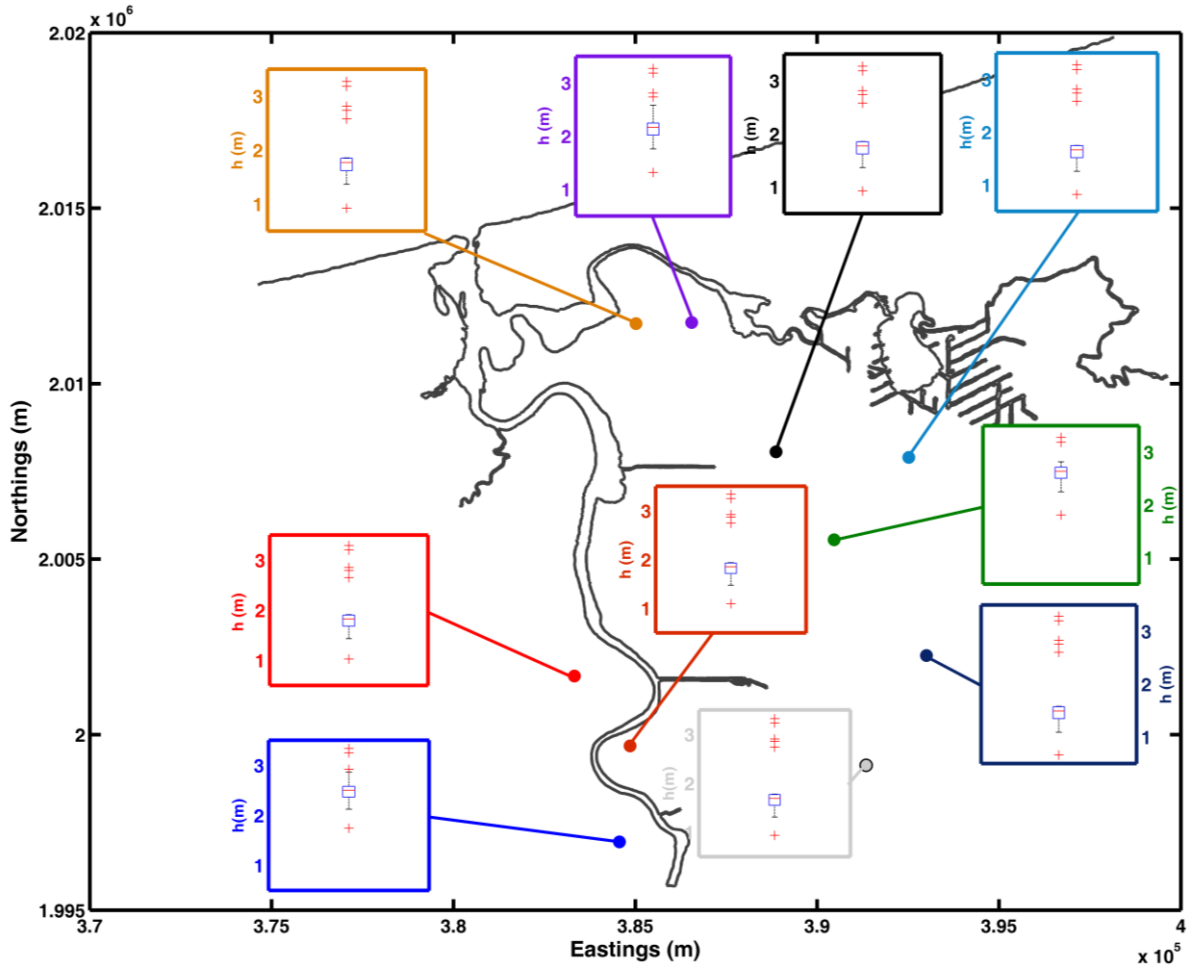
Figure 8. Data vs. model comparison of flood extent; a) Probabilistic flood map derived from the ensemble runs with the hydrodynamic model; b) Infrared SPOT image corresponding to the 15th November 2009.



2
3
4
5
6
7
8
9
10

Figure 9. a) Maximum-flooded area vs. peak discharge estimated for all 31 hydrodynamic simulations of the 2009 flood event; b) Histogram of peak discharges; c) Histogram of estimated size of maximum-flooded area.

1



2

3

4

5

6

7

8

9

10

11

12

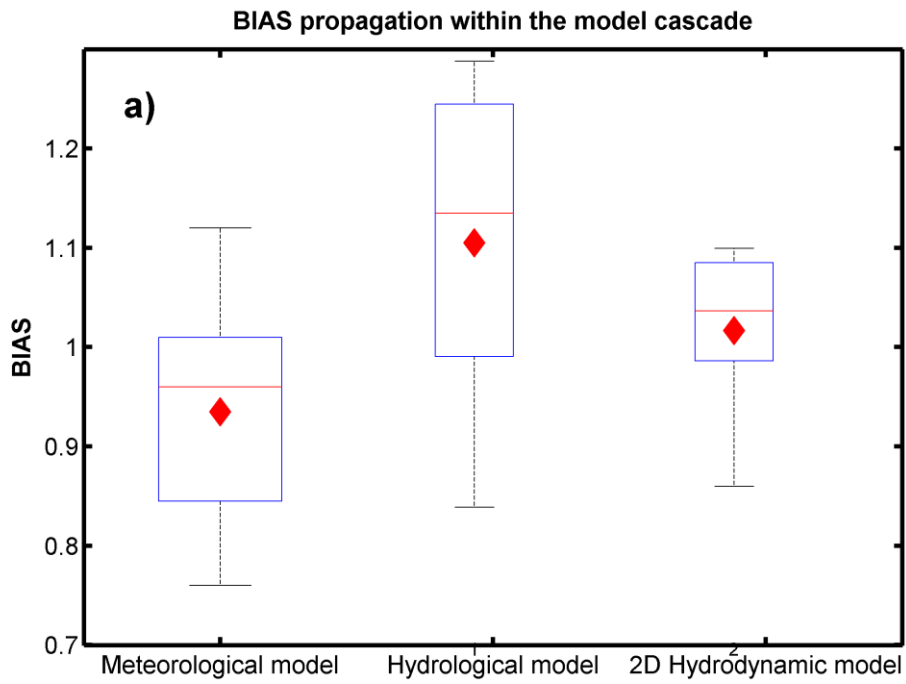
13

14

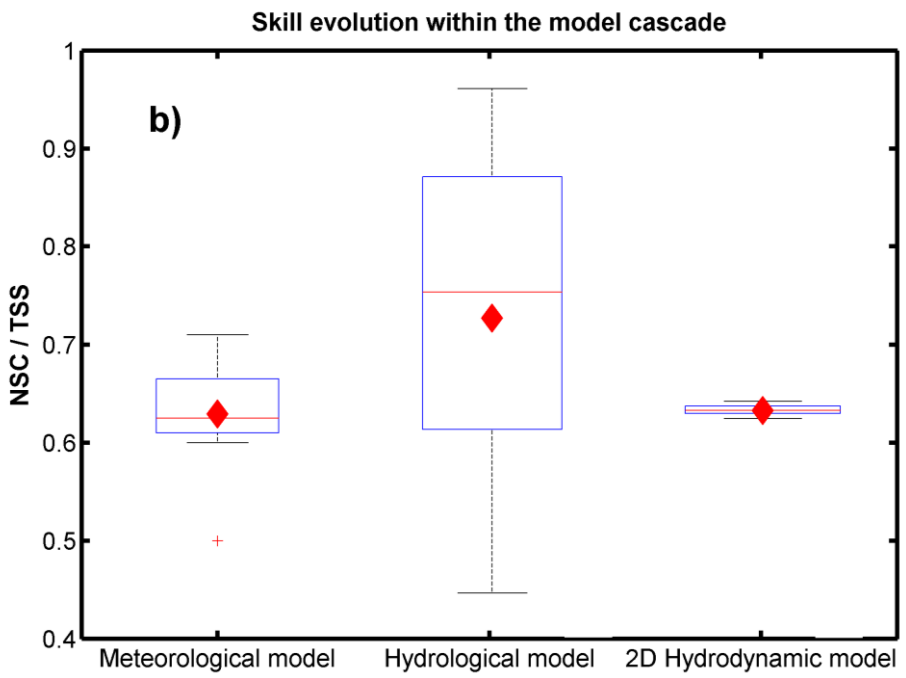
15

Figure 10. Estimated maxima inundation depths at different locations within the floodplain. Red line represents the median. Bars correspond to the standard deviation. Upper and lower limits of the box are the values of the 25th and 75th , respectively. Crosses depict outliers.

1



2



3

4

5

Figure 11. a) BIAS and b) Skill propagation within the model cascade (meteorological-hydrological-hydrodynamic); diamonds: corresponding ensemble mean value.